National Technical University of Athens
School of Chemical Engineering

Postgraduate Studies Program
"Computational Mechanics"
Direction: Fluid Mechanics

MASTER'S THESIS

Modelling Pharmaceutical Capsule Filling Processes

Nikoletta Patsaki

Supervisors:

Prof. Chris T. Kiranoudis,
Prof. Nicholas C. Markatos
School of Chemical Engineering, NTUA, Greece

Dr.Charles Radeke,
Research Center Pharmaceutical Engineering, RCPE, Austria

March 2014

A B S T R A C T

Evaluation of the factors contributing to the uniformity of the fill weight of pharmaceutical capsules, obtained by automatic capsule filling machines, has been a challenge over the years. One of these factors is the uniformity of the powder bed, from which the dose to be transferred in the capsule body, is obtained. The kinetic energy fluctuations occurring during the process of capsule filling on the powder bed, lead to fluctuations in the bulk density of the powder at the sampling areas, affecting the uniformity of the whole powder bed after consecutive sampling. A simulation of the accurate capsule filling process, performed by an MG2 capsule filling machine, was carried out at the Research Center Pharmaceutical Engineering (RCPE), in Graz, Austria.

The first objective was the study of some of the operational parameters affecting the energy fluctuations on one representative sampling volume, as well as the volume number density of the sampled powder, in a dosing chamber of set size. The factors examined were two equipment parameters: the sampling velocity of the dosator and the size of the dosing chamber. Three results were obtained: 1. An increase in the dosator speed, results in an increased volume number density of the dosage. 2. The total kinetic energy of the particles on one sampling volume, increases with the dosator speed. 3. While decreasing the size of the dosing chamber, the total kinetic energy on the sampling volume increases. These results allow recommendations on the acceptable limits of the sampling velocities and how different dosing chamber sizes, affect the kinetic energy within the powder bed.

The second objective of this thesis was to achieve the simulation of the accurate amount of particles contained in one sampling volume of the rotary container. This was achieved by using an in-house code called Graz Rutgers Particle Dynamics (GRPD). GRPD is a code based on the Discrete Element Method (DEM), written in the programming language C and the Compute Unified Device Architecture (CUDA), which is a parallel computing platform running on Graphics Processing Units (GPUs). Compared to existing commercial software that are able to simulate granular systems, GRPD is capable of simulating up to millions more particles depending on the application. In the scope of this work, 4 million spherical particles were simulated in a smaller section (one sampling volume), of the powder container. The diameter distribution of the particles simulated, matched the actual particle size distribution of the product Lactohale 100, thus achieving the realistic simulation of this granular system.

Π Ε Ρ Ι Λ Η Ψ Η

Η αξιολόγηση των παραγόντων που συνεισφέρουν στην ομοιομορφία του βάρους πλήρωσης φαρμακευτικών καψακίων, που λαμβάνονται από αυτόματες μηχανές πλήρωσης καψακίων, έχει υπάρξει πρόκληση ανά τα έτη. Ένας από αυτούς τους παράγοντες είναι η ομοιομορφία του στρώματος κόνεως, από το οποίο λαμβάνεται η δόση που μεταφέρεται στα καψάκια. Οι ενεργειακές διακυμάνσεις που σημειώνονται κατά τη διαδικασία της αυτόματης πλήρωσης καψακίων στο στρώμα κόνεως, οδηγούν σε διακυμάνσεις στην φαινόμενη πυκνότητα της κόνεως, στις περιοχές δοσοληψίας, επηρεάζοντας την ομοιομορφία του συνολικού στρώματος κόνεως, μετά από συνεχείς δοσοληψίες. Η προσομοίωση της ακριβής διαδικασίας πλήρωσης καψακίων, όπως εκτελείται από μία αυτόματη μηχανή πλήρωσης καψακίων MG2, πραγματοποιήθηκε στο ερευνητικό κέντρο Research Center Pharmaceutical Engineering (RCPE), στο Graz της Αυστρίας.

Ο πρώτος στόχος ήταν η διερεύνηση ορισμένων από τις λειτουργικές παραμέτρους που επηρεάζουν τις ενεργειακές διακυμάνσεις, σε έναν αντιπροσωπευτικό όγκο δοσοληψίας, καθώς επίσης και την σωματιδιακή πυκνότητα της λαμβανόμενης κόνεως, εντός δοσιμετρικού θαλάμου προκαθορισμένου μεγέθους. Οι παράγοντες που μελετήθηκαν ήταν δύο παράμετροι εξοπλισμού: η ταχύτητα δοσοληψίας και το μέγεθος του δοσιμετρικού θαλάμου. Δόθηκαν τρία αποτελέσματα: 1. Άυξηση στην ταχύτητα του δοσομετρητή, καταλήγει σε αυξημένη σωματιδιακή πυκνότητα δόσης. 2. Η συνολική κινητική ενέργεια των σωματιδίων σε έναν όγκο δοσοληψίας, αυξάνεται ανάλογα με την ταχύτητα του δοσομετρητή. 3. Μειώνοντας το μέγεθος του δοσιμετρικού θαλάμου, η συνολική κιν-

ητική ενέργεια στο όγκο δοσοληψίας, αυξάνεται. Τα αποτελέσματα αυτά επιτρέπουν συστάσεις σχετικά με τα αποδεκτά όρια των ταχυτήτων δοσοληψίας και πώς τα διαφορετικά μεγέθη δοσιμετρικού θαλάμου, επηρεάζουν την κινητική ενέργεια στο στρώμα κόνεως.

Ο δεύτερος στόχος της παρούσας εργασίας, ήταν να επιτευχθεί η προσομοίωση του ακριβή αριθμού σωματιδίων, εντός ενός όγκου δοσοληψίας επί του περιστροφικού δοχείου. Αυτό επιτεύχθηκε με τη χρήση ενός κώδικα που ονομάζεται Graz Rutgers Particle Dynamics (GRPD). Το GRPD είναι ένας κώδικας βασισμένος στην μέθοδο διακριτών στοιχείων (DEM), γραμμένος στην γλώσσα προγραμματισμού C και στην Compute Unified Device Architecture (CUDA), η οποία είναι μία πλατφόρμα παράλληλου προγραμματισμού που εκτελείται σε Graphics Processing Units (GPUs). Σε σύγκριση με υπάρχοντα εμπορικά υπολογιστικά πακέτα ικανά να προσομοιώσουν κοκκώδη συστήματα, το GRPD είναι ικανό να προσομοιώσει μέχρι και εκατομμύρια περισσότερα σωματίδια, αναλόγως την εφαρμογή. Σε αυτήν την εργασία, έγινε προσομοίωση 4 εκατομμυρίων σφαιρικών σωματιδίων σε έναν μικρότερο τομέα (όγκος δοσοληψίας), του δοχείου κόνεως. Η κατανομή διαμέτρων των σωματιδίων που προσομοιώθηκαν, ήταν σύμφωνη με την κατανομή μεγέθους των σωματιδίων του προιόντος Lactohale LH100, οπότε και επιτεύχθηκε η ρεαλιστική προσομοίωση του κοκκώδους αυτού συστήματος.

A C K N O W L E D G E M E N T S

I would like first of all, to express my gratitude and appreciation to my advisor Dr. Charles Radeke for his guidance and encouragement through all these months. He has been a great mentor figure to me, both as a scientist and as a person. I would also like to thank my supervisors from National Technical University of Athens, professor Nicholas Markatos and professor Chris T. Kiranoudis for the priceless knowledge they provided me through post-graduated courses and for giving me the opportunity to realize this master's thesis.

I would especially like to thank Mag. Eva Faulhammer and Dr. Markos Llusa for their advice and information, valuable for this work. I also feel especially thankful to DI Georg Scharrer, for the opportunities he gave me while being a member of his team at Research Center Pharmaceutical Engineering, RCPE.

My friends both in Graz and in Athens had been a great support network for me, always welcoming me and supporting me both in fun times and in more stressful situations.
I would like to express my eternal love and gratitude to my family for their warmness, support and kindness through every step in my life.

Contents

List of Figures

1 Introduction

Particulate systems are of great significance for industrial processes. Their importance derives from the fact that most of the raw materials used by industries to manufacture final products, are granular materials. They are encountered in a big range of different industrial disciplines, such as pharmaceutics, agriculture, mining, food and cosmetics production, chemical processing and environment. Lack of research on the micro-mechanical phenomena occurring within particulate materials, as well as on their often multiphase nature, frequently leads to poor manufacturability into final products. In order to overcome such production problems, it is crucial, that the discrete nature of particulate systems is under consideration.
The discrete element method (DEM), is a well established computational method, able to simulate processes involving particulate matter, while tracking the motion of each individual particle in the system, as well as considering inter-particle and particle-boundaries interactions.

In the scope of this thesis, a particulate process from the pharmaceutical industrial sector is simulated. The process of capsule filling performed by an automatic dosator -principle machine. As a first approach, the objective here was to accurately simulate the machine components of the capsule filling machine used, and the real number and size of particles of the pharmaceutical powder Lactohale LH100 and using DEM and parallel programming to study the effect of some of the process parameters to the kinetic energy on the powder bed and the volume number density of the dose obtained. This could be used later as a basis for a second approach,

including more of the material properties, for further investigation, for example on the mechanical stresses inside the dosing tube, or even multiphase approaches.

Chapter two, contains an overview of capsule filling, descriptions of the machine parts such as the dosator and the process steps performed by a capsule filling machine.

In chapter three, the theoretical background is defined, including granular materials and how they can be simulated, and an analytic description of the discrete element method (DEM) and its fundamental equations.

Chapter four, describes the code used for the current simulation, and what was defined while setting up the simulation.

In chapters five the results are given and analyzed and further recommendations and a conclusion is reached in chapter six.

2 Background

2.1 Capsule filling

Capsule filling processes are growing in importance for the pharmaceutical industry, who is in a constant research, for the least time consuming procedures for drug development. In comparison to tablets, hard capsules are simpler to produce. Specifically, during formulation development in the early stages of a clinical trial of a new drug, capsules require much less excipients than tablets, or in some cases, only the API (Active Pharmaceutical Ingredient) itself. Moreover, in capsule filling processes, some of the steps that are always present in tableting, could be avoided, such as granulation, drying, sieving, addition of lubricants and compression. Capsules can also provide protection for sensitive API's and they can serve as an alternative for API's that are not compressible to the extend required for tableting, or API's with such properties that restrict combination with other excipients. Industries are then allowed, to introduce a new drug to the market, faster and in some cases safer. Some disadvantages are, that the manufacturing process of capsules, is more expensive than tableting, as well as that some API's are unsuitable for capsule filling due to physical properties, and in some cases, delivering the whole predicted dose of drug into the hard capsules, might not be achieved, which may lead to incomplete or empty capsules.

Encapsulation processes could be done on manual, semi-automatic and automatic machines. At the beginning of the 20th century, the first semi- automatic filling machines were designed and used in an industrial scale. Excessive use and research, led to the first automatic machine, designed by Arthure Colton in 1950. A fundamental component for every filling machine, is its dosing system. Depending on the kind of their dosing mechanism, filling machines are categorized into dependent-type, or independent-type machines[1]. Dosing is performed directly into the two-piece hard capsules on the first category, while on the second, a plug with the appropriate dose is formed, outside of the capsule body and then it's inserted into the capsule. Automatic, independent-type filling machines, are the most widespread and they are governed by two main dosing rules for filling capsules with powder, the tamping (dosing disc) system and the dosator system. Their main difference is in the formation of the powder plug. The dosing disc system, requires numerous consecutive actions while on the dosator-based machines, plug formation is achieved by a single movement, performed by a piston. This study is focused on the principles of the dosator system. The main task of the dosator is to transfer accurate doses of powder into hard gelatin capsules. In the process of capsule filling, all the factors affecting the attainment of such accurate fill weights, have to be taken into account.

2.2 MG2 dosator filling machine

2.2.1 The dosator

A variety of different dosator systems have been manufactured, such as the MG2, Romaco and IMA-Zanazi capsule filling series. Although the simulation was based on the MG2 dosator principles, the results could also be applied to other dosator systems, since despite their differences, they share common principles on their operation and similar design features. Design and operational description of the dosator, as well as the process of the MG2 capsule filling lab scale (LABBY) will be analyzed here.

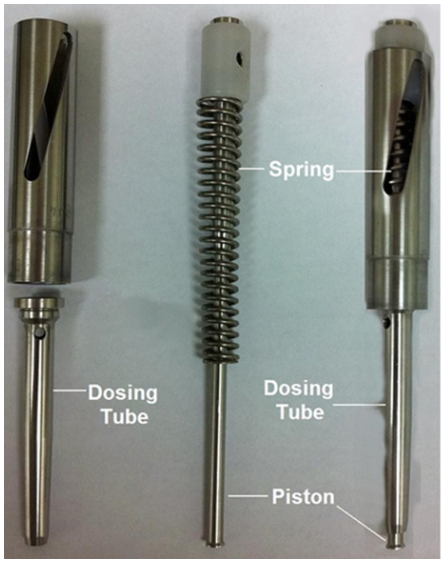

Figure 2.1: Standard dose MG2 dosator

Figure 2.2: Low dose MG2 dosator

As observed in figure 2.1 and figure 2.2, the dosator consists of three main stainless steel parts. The dosing tube, the piston and a spring. While in intermittent motion filling machines, the piston is driven hydraulically or pneumatically, in automatic filling machines it is driven by the spring. The piston is placed inside the dosing tube, demonstrating reciprocating motion, assisted by the spring. The movement of the piston, defines the space of the dosage chamber, and consequently the volume of the powder plug to be formed, it is also responsible for the compaction of the powder inserted to the the chamber and it is used for the ejection of the formed plug into the capsule. This will be better understood later, in the description of the filling process steps.

There are two different MG2 dosator types. The standard dose and the low dose dosators (figure 2.1 and 2.2 respectively). This categorization occurs from the different sizes of capsules that are manufactured and this is because the required dose of powder in a capsule, varies depending on the application. In both cases, a hole is designed at the upper part of the dosing tube. This opening allows the air that is displaced while powder is entering the tube, to escape. As one can observe in figures 2.1, 2.2, the low dose is much smaller than the standard dose dosing tube, with regard to their hight and internal diameter (as internal diameter is defined, the lowest internal diameter of the dosing tube).The internal geometry of the dosing tube is a cylinder, while the outer geometry is a cylinder with a conical lower part. After the dosator collects the powder, it ejects it into the capsule body. The capsule body is placed into a capsule body bush. The dosator lines up with that bush. The conical shape of the lower part of the dosator fits better than a cylindrical shape on the bush's opening. One example that the low dose dosator is used, is for the production of dry powder inhaler (DPI) capsules, which can be then placed in inhalation carriers. Very small doses, as for example required for inhalation purposes, are filled into capsules by the low dose dosator which consequently comes in smaller sizes than the standard dose dosators. In the current simulation, a low dose dosator of internal diameter 3.4 mm (capsule size 3) was modeled.

2.2.2 MG2 Capsule filling process steps

The capsule filling process which was simulated, is carried out at the MG2 capsule filling lab scale(LABBY). In the laboratory of the Research Center Parmaceutical Engineering RCPE, measurements of the dimensions of the parts of the LABBY that were used for the simulation, were performed and the steps of the filling process were observed.

The following image, pictures the sequence of operations performed by the MG2 PLANETA capsule filling machine:

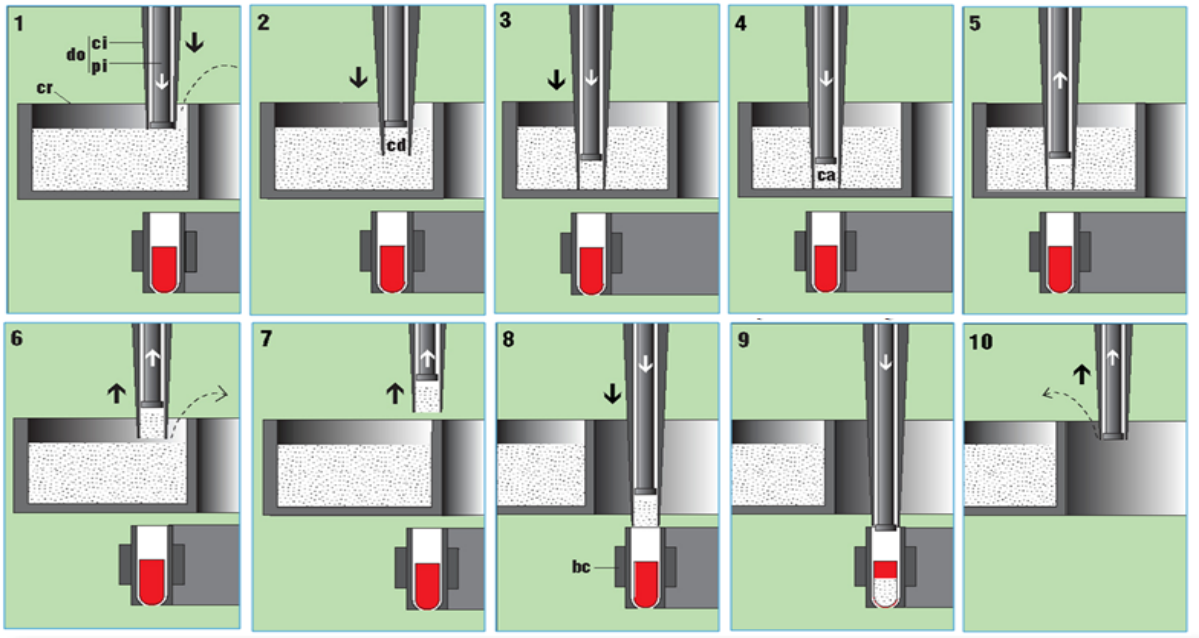

Figure 2.3: Capsule filling process steps - MG2 PLANETA

Figure 2.4: MG2 capsule filling lab scale (LABBY)

Figure 2.3 pictures the ten steps of the filling process, as described in the customers leaflet for the MG2 PLANETA capsule filling machine. In stage 1, the dosator travels downwards until the surface of the powder bed. In stage 2, the size of the dosing chamber is defined, by pausing the piston's descent, while the tube is lowered until a specific position inside the powder bed, depending on the desirable chamber size. In stage 3, the chamber, as defined in stage 2, is filled with the dose, after the dosator reaches the bottom of the vessel. The compaction stage 4, is optional and applied if the properties of the powder require it. In stages 6,7, 8 and 9 the dosator is transferred at the opening of the capsule body bush and the piston applies sufficient force vertically to the plug in order to eject it into the capsule. In stage ten the dosator resets to its initial position to begin another sampling.

This process reproduces up to 3.500 capsules per hour, when performed by the MG2 LABBY capsule filling machine.

The lab-scale (LABBY) capsule filling machine, has only one dosator, sampling repeatedly on different sampling areas in the container, while the PLANETA capsule filling machine has numerous dosators. The dosators are placed in a turret, which rotates horizontally. The rotary container is below the turret and it rotates around a different center than the turret. No lateral movement between the dosator and the powder bed should be introduced while the dosator is lowered towards the container. After the dosator collects the desirable dose of powder, it has to retain it during its way towards the capsule body. If the powder properties allow this, it can be retained in the dosator without any intervention, but frequently, compression (stage 4) is required. In the compression stage, the piston compresses the powder by applying a vertical compressive stress which, due to increased friction between the powder and the dosing tube's internal walls, leads to the formation of an arch, that allows retention of the powder in the dosing chamber. Compression often fails to retain the powder, because retention depends on numerous factors, some of them known and some still under research. In the ejection stage, the force applied by the piston has to overcome these frictional forces, so that the plug can be ejected. Creating and retaining a uniform powder bed, is very important for attaining accurate fill weights but also for the retention of the powder in the dosator.

3 Theoretical Framework

3.1 Granular Material

3.1.1 Definition - Consideration

Figure 3.1: Granular materials

Granular materials consist of discrete solid, macroscopic particles, most frequently in large numbers. Sand, coffee, rice, coals, grains in silos, are some examples of granular materials, differing in particle size, shape and number. Pharmaceutical powders and generally powders, are a special category of granular materials, in terms of their

cohesive behavior due to smaller particle sizes. The advantages and disadvantages of existing granular material physical descriptions, deduced from laws of continuum mechanics have been considered under a lot different points of views [2, 3, 4, 5, 6, 7]. Some even characterized granular materials, as a distinct state of matter, after gases, liquids and solids .Their wide range of applications such as in pharmaceuticals, chemical processing, mixing, mining and agriculture, make the study of their behavior an important matter of research. Granular materials display different behavior depending on the application and their properties, making establishment of general rules difficult. This is particularly inconvenient for industries, that need such rules in order to apply them in automatic procedures for handling the particulate material of interest. Experimental research of every application of every individual material, could require expensive equipment and time consuming procedures and yet not guarantee a useful result. Researchers turn more and more into the development and use of modeling tools, because computer simulation allows altering material, process and equipment parameters, numerous times, easily and with almost no cost. Unfortunately this often comes with the prize of various computational limitations.

3.1.2 Modeling Granular Materials

There are various numerical methods and algorithms, developed for solving and analyzing problems involving granular materials. They could be shorted into two basic

categories. Computational methods and tools on the first category, model granular flow with a continuum mechanics approach, at a macroscopic scale, while those on the second, are based on the micro mechanical behavior of granular materials. This categorization on these two different granular material mechanical approaches was first introduced in [8]. They have different theoretical backgrounds and disciplines and each presents both advantages and limitations.

The Finite Element method (FEM) and the Finite Volume Method (FV), used excessively in Computational Fluid Dynamics (CFD), are some of the most representative methods of the first category. Applied to a variety of simulation software, they can simulate granular flows successfully but under assuming the material as a continuum and introducing material parameters (internal variables), to describe elasticity, plasticity, visco- plasticity or other material properties. In general, granular materials are described by discontinuous, heterogeneous and anisotropic behavior. In contrast, continuum mechanics fundamental laws, are built under assumptions of continuity, homogeneity and isotropy [9]. In order to regard granular material under such assumptions, it is often necessary, to convert the micro-mechanical properties of the granular material into macroscopic terms, thus some inter-particle interactions are not taken into account. This limitation excludes a big variety of industrial applications from being examined under such simulation approaches. In addition, the determination of constitutive laws, is challenging, and a lot of equations need to be solved, in frequently complex computational domains.

The micro mechanical methods, composing the second category, derived from the distinct element method proposed for the first time by Cundall [10]. Later this method was introduced into a computational tool [11], and it was used in [12, 13]. The distinct element method by Cundall, the generalized discrete element method, proposed by Hocking, Williams and Mustoe [14] and the discontinuous deformation analysis (DDA), proposed by Shi [15], are all methods of the discrete element method (DEM) family. The discrete element method, instead of using a constitutive model, it tracks the positions, velocities and accelerations, of each individual particle, over time. It takes into account the micro - scale interactions of particles within the material, the particle-particle and particle-boundary contact forces and the body forces such as gravity. The material properties introduced in a DEM code, by this microscopic approach, allow a more accurate simulation of phenomena such as segregation, breakage, agglomeration or the effect of non shperical particles, which are not easy to implement with continuum mechanical modeling. The challenge is the simulation of the accurate number of particles within a granular system, and at the same time, simulating the process of interest, in an acceptable simulation time. This limitation derives from todays limited computational resources for such large-scale calculations.

Techniques in both categories can be combined, for solving problems involving granular materials and fluids. Many CFD-DEM coupled software have been developed for such multiphase approaches [16, 17, 18]

3.2 Discrete Element Method (DEM)

In this work, the soft-sphere DEM approach is employed and the process it follows, as well as its theoretical background will be analyzed here.

3.2.1 DEM calculation cycle

The Discrete element method, follows a dynamic (time driven) process for computing the motion and effect of a large particle system. The general idea, is simple. Computing the forces acting on each particle, allows to reduce the problem to only the integration of Newton's second law of motion, to update velocities and displacements of each particle. The calculation cycle that a DEM code follows, is reviewed on the following flowchart:

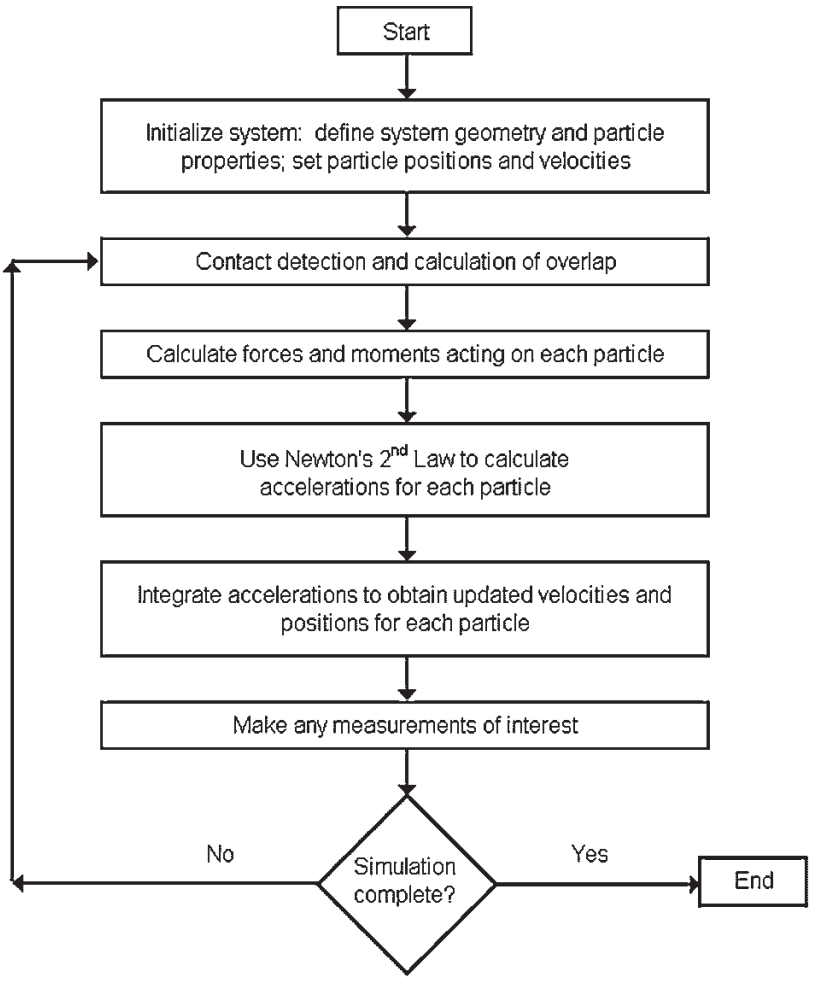

Figure 3.2: DEM calculation cycle . Flowchart from publication [19].

During the basic cycle of a DEM cycle, at first, the user defines the desired particle parameters, to achieve a realistic representation of the material. Some of the parameters that could be defined at this step, have been reviewed in [20]. Among the most important are, the number of particles, particle diameter distribution, particle shape

(for large number of particles, spherical shape is the most convenient), coefficients of static and rolling friction, particle coefficient of restitution, packing density, porosity and spring stiffness. The spring stiffness values allow particles to deform by slightly overlapping when they collide with surrounding particles or walls. Then the geometry of the system is described, and in case of the process to be simulated, involves industrial equipment or machinery, its geometry and motion are defined here. The code then generates initial position coordinates and velocities for introducing the desired number of particles with the previously defined properties, inside the defined geometry.

In the next step, the calculation cycle begins. The contact points between particles and particles to boundaries are detected and stored for the next step. The number of contacts of one particle, is called coordination number. Also, the code calculates the overlapping value at each contact point. In the second step, the total force is calculated. Specifically, when particles are in contact, normal and tangential contact forces are introduced and summing them up with the body forces acting on them, such as gravity, the total force on each particle is calculated. There are several contact models for the calculation of contact forces, here the linear spring dashpot model is used. In the third step accelerations for each particle are obtained by Newton's second law of motion. By integration of Newton's second law of motion, the position and velocity updates of each particle are calculated. The cycle repeats until the end of the simulation.

3.2.2 DEM theoretical background

Consider two colliding particles i and j:

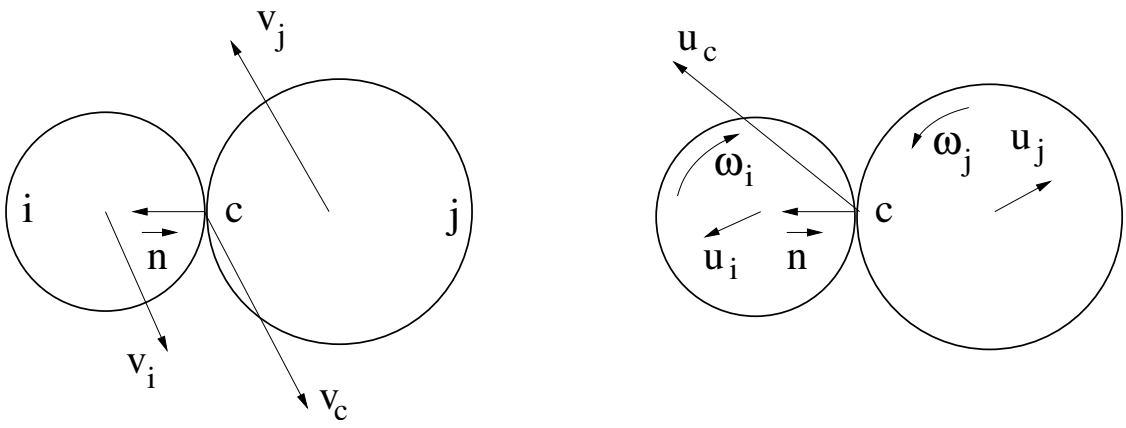

Figure 3.3: Two particles before and after collision.

The coefficient of restitution ϵ_{ij} is given by :

$$\epsilon_{ij} = -\frac{u_1 - u_2}{v_1 - v_2} \tag{3.1}$$

Where,

v_1, v_2 the initial velocities of the first and second particle respectively, before impact

u_1, u_2 the final velocity of the first and second particle respectively, after impact.

The relative velocity at the contact point c, is given by :

$$\vec{v}_c = (\vec{v}_i - \vec{v}_j) - (r_i\vec{\omega}_i + r_j\vec{\omega}_j) \times \vec{n} \tag{3.2}$$

Where,

r_i, r_j the radius of the i and j particle respectively,

ω_i, ω_j the angular velocity of the i and j particle respectively, after impact.

$\vec{n}$ the normal vector

Newton's second law of motion in vector form:

$$\vec{F} = m\ddot{\vec{x}} \tag{3.3}$$

Where, $\vec{F}$ is the force applied, m the particle mass: $m = \rho\frac{4}{3}\pi r^3$ (ρ is the material density), and $\ddot{\vec{x}}$ the acceleration, expressed as the second order derivative of the position vector $\vec{x}$

If the particles deform after collision, the overlap δ_{ij}, is expressed by :

$$\delta_{ij} = (r_i + r_j) - |\vec{x}_i - \vec{x}_j| \tag{3.4}$$

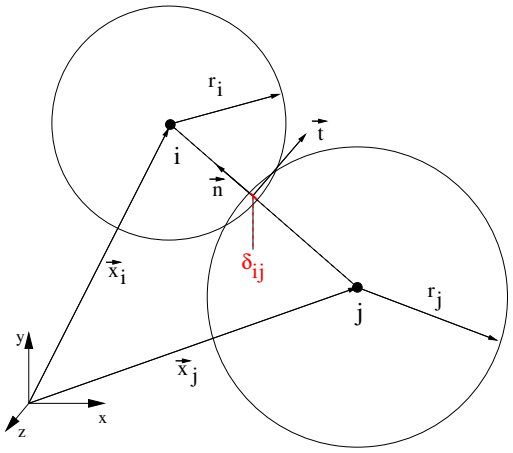

Figure 3.4: Overlapping particles.

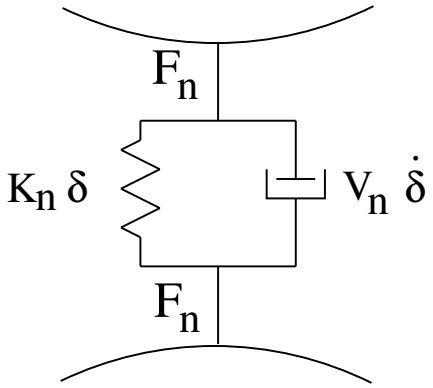

Figure 3.5: Spring - Dashpot Model.

and the relative impact velocity (first order time derivative of overlap), is:

$$\dot{\delta}_{ij} = -(\vec{v}_i - \vec{v}_j) \cdot \vec{n} \tag{3.5}$$

The normal force between two particles i, j, in the Linear Spring Dashpot model, is:

$$F_{n_{ij}} = K_n \delta_{ij} + V_n \dot{\delta}_{ij} \tag{3.6}$$

Where, K_n is the linear spring stiffness, V_n the damping coefficient and $\vec{n}$ the normal vector.

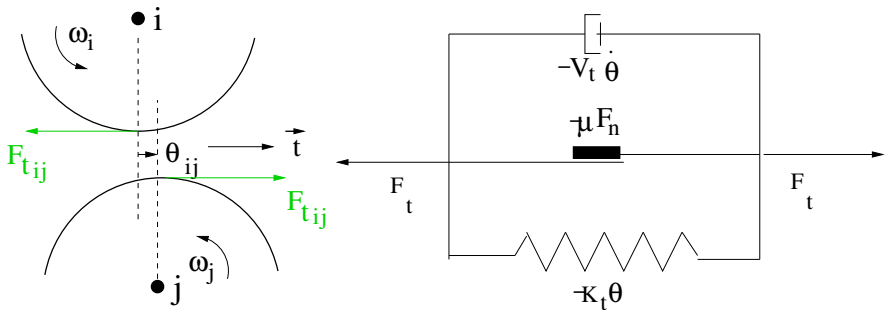

Figure 3.6: Tangential velocity and Spring-Dashpot model in the tangential direction, respectively.

The tangential velocity at the contact point, is the projection of the relative velocity $\vec{v}_c$, in the tangent plane:

$$\dot{\theta}_{ij} = \vec{v}_c \cdot \vec{t} = [(\vec{v}_i - \vec{v}_j) - (r_i \vec{\omega}_i + r_j \vec{\omega}_j) \times \vec{n}] \cdot \vec{t} \tag{3.7}$$

The tangential force is calculated by:

$$F_{t_{ij}} = -K_t\theta_{ij} - V_t\dot{\theta}_{ij} - \mu F_{n_{ij}} \tag{3.8}$$

Where, K_t is the tangential spring stiffness, V_t the damping coefficient, $\vec{t}$ the tangential vector and μ, the friction coefficient.

Also the body forces due to gravity $\vec{g}$ and viscosity V_g are:

$$\vec{F}_{i_{grav}} = m_i\vec{g} \tag{3.9}$$

$$\vec{F}_{i_{Vg}} = -V_g\dot{\vec{x}}_i \tag{3.10}$$

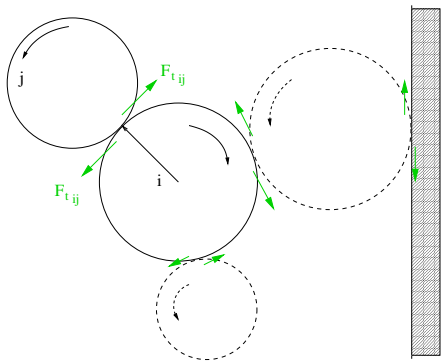

Figure 3.7: Particle-Particle and Particle-Wall tangential forces and moments.

By the circular equations of motion, the angular torque is:

$$\vec{M} = \Theta\dot{\vec{\omega}} \tag{3.11}$$

Where the moment of inertia of the particle i, is:

$$\Theta_i = \frac{2}{5} m_i r_i^2 \tag{3.12}$$

And the torque of particle i :

$$\vec{M}_i = \sum_j \vec{r}_i \times \vec{F}_{t_{ij}} \tag{3.13}$$

Particle - Wall contact

Particle i -Wall $\omega(j)$, overlap:

$$\delta_{i,\omega(j)} = r_i - |\vec{x}_i - \vec{x}_{\omega(j)}| \tag{3.14}$$

Relative impact velocity:

$$\dot{\delta}_{i,\omega(j)} = -(\vec{v}_i - \vec{v}_{\omega(j)}) \cdot \vec{n} \tag{3.15}$$

Tangential velocity:

$$\dot{\theta}_{i,\omega(j)} = \vec{v}_c \cdot \vec{t} = [(\vec{v}_i - \vec{v}_{\omega(j)}) - r_i\vec{\omega}_i \times \vec{n}] \cdot \vec{t} \tag{3.16}$$

normal forces of particle i in contact with a wall $w(j)$:

$$\hat{F}_{n_{i,\omega(j)}} = K_n\delta_{i,\omega(j)} + V_n\dot{\delta}_{i,\omega(j)} \tag{3.17}$$

Normal force acting on a wall:

$$F_{n_{i,\omega(j)}} = \sum_i \hat{F}_{n_{i,\omega(j)}} \tag{3.18}$$

Tangential Force:

$$F_{t_{i,\omega(j)}} = -\bar{K}_t\theta_{i,\omega(j)} - \bar{V}_t\dot{\theta}_{i,\omega(j)} - \bar{\mu}F_{n_{i,\omega(j)}} \tag{3.19}$$

Kinetic Energy

The total kinetic energy of a particle i, is the sum of its center of mass translational kinetic energy, and rotational energy:

$$E_{i,tns}(t) = \frac{1}{2} m_i v_i^2(t) \tag{3.20}$$

$$E_{i,rot}(t) = \frac{1}{2} \underbrace{\frac{2}{5} m_i r_i^2}_{\Theta_i} \omega_i^2(t) \tag{3.21}$$

$$E_{i,kin}(t) = E_{i,tns}(t) + E_{i,rot}(t) = \frac{1}{2}(\Theta_i \omega_i^2(t) + m_i v_i^2(t)) \tag{3.22}$$

And the total kinetic energy of the particle system:

$$E_{kin}(t) = \sum_i E_{i,kin}(t) \tag{3.23}$$

,is the sum of the kinetic energy of each particle i

Potential Energy

The total potential energy of a particle i, is the sum of its spring potential energy, and gravitational potential energy:

$$E_{i,spr}(t) = \frac{1}{2}\sum_{j} K_n \delta_{ij}^2(t) + \frac{1}{2}\sum_{j} K_t \theta_{ij}^2(t) \tag{3.24}$$

$$E_{i,grav}(t) = m_i g z_i(t) \tag{3.25}$$

Where, z_i, the z coordinate of the particle i.

$$E_{i,pot}(t) = E_{i,spr}(t) + E_{i,grav}(t) = \frac{1}{2}(\sum_{j} K_n \delta_{ij}^2(t) + \sum_{j} K_t \theta_{ij}^2(t)) + m_i g z_i(t) \tag{3.26}$$

And the total potential energy of the particle system:

$$E_{pot}(t) = \sum_{i} E_{i,pot}(t) \tag{3.27}$$

,is the sum of the potential energy of each particle i

4 Simulation

4.1 The GRPD code

In this work the Graz-Rutgers Particle Dynamics (GRPD) code, proposed in [21], was used for the simulation of a capsule filling process as described in chapter 2. It is an in-house DEM code, written in CUDA C/C++ . Compute Unified Device Architecture (CUDA), invented by NVIDIA, is a parallel computing architecture, implemented by GPUs. The GPU is interacting with the Open Graphics Library (OpenGL), for the visualization of the simulation. GPU computing with CUDA, allows dramatic computational speedup in comparison to CPU computing.

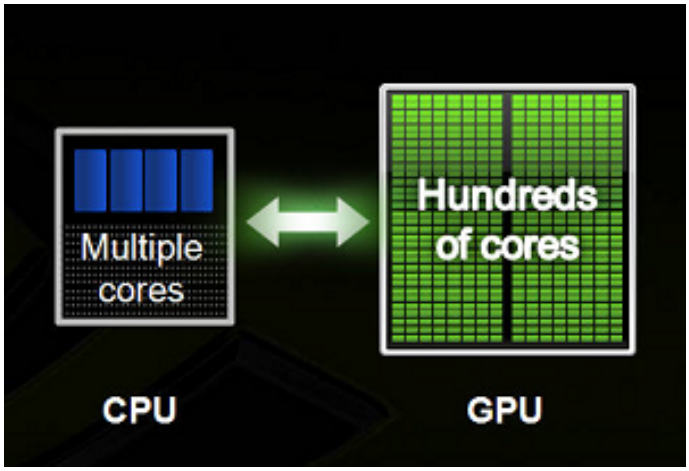

Figure 4.1: CPU vs GPU.

The tasks of a DEM cycle described in paragraph 3.2.1, are independent tasks, thus easy to parallelize. The reason is that the equations described in 3.2.2 for each particle, can be executed simultaneously, by distributing them on multiple microprocessors. Memory size of the Graphics Processor used, is one of the factors that defines the capability of the code to generate and process a large number of particles. For the current simulation, an NVIDIA graphics card with 4 GB of memory was installed.
In order to execute the steps of a DEM cycle (paragraph 3.2.1), GRPD uses some specific tecqniques:

- Generate particles / sphere packing algorithms:

  After defining the desired particle and geometry parameters in input files, GRPD generates the predefined number of particles using the sedimentation algorithm. The sedimentation algorithm is a sphere packing algorithm, proposed by Jodrey and Tory [22]. Particles falling in the gravitational field, are introduced in the rotary container. Other sphere packing algorithms have been proposed, such as the force-biased algorithm [23, 24].

- Contact detection / neighbor lists:

  The contact detection step could be rather computationally expensive. GRPD

uses a cell structure method [25], for a fast neighbor detection, by dividing the simulation domain into sub-cells. Among other neighbor detection methods, is the Verlet neighbor list also described in [25].

- Calculate forces / contact models:

  GRPD uses the Linear-Spring-Dashpot Model (LSD), for the calculation of forces from displacements. It is a soft sphere contact model, proposed in [26, 27]. The theory of LSD, was described in paragraph 3.2.2. Other contact models include the non linear Hertzian-Spring-Dashpot (HSD), described in [28, 29].

- Numerical Integration:

  For time integration of Newton's second law of motion, for displacement updates, an explicit integration algorithm is used, the Verlet integration scheme. Small time steps are required for maintaining stability. After obtaining displacements for the new time step, velocity updates are obtained by central differences.

4.2 Simulation Setup

The geometry of the equipment parts of the MG2-LABBY capsule filler, necessary for the simulation, was specified. Specifically, the dimensions of the rotary container and the low-dose dosator of 3.4 mm diameter, were defined within the code.

Figure 4.2: The rotary container-MG2 LABBY

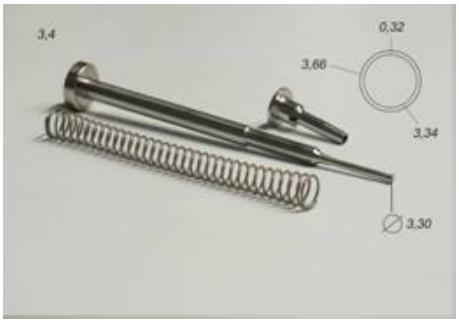

Figure 4.3: Low-dose dosator (3.4 mm)

Parameter	Dimension
Container Outer diameter	27.6 cm
Dosing tube Inner diameter	3.4 mm
Dosing tube Outer diameter	4 mm
Piston diameter	3.3 mm

Table 4.1: Dimensions of the rotary container and the dosator

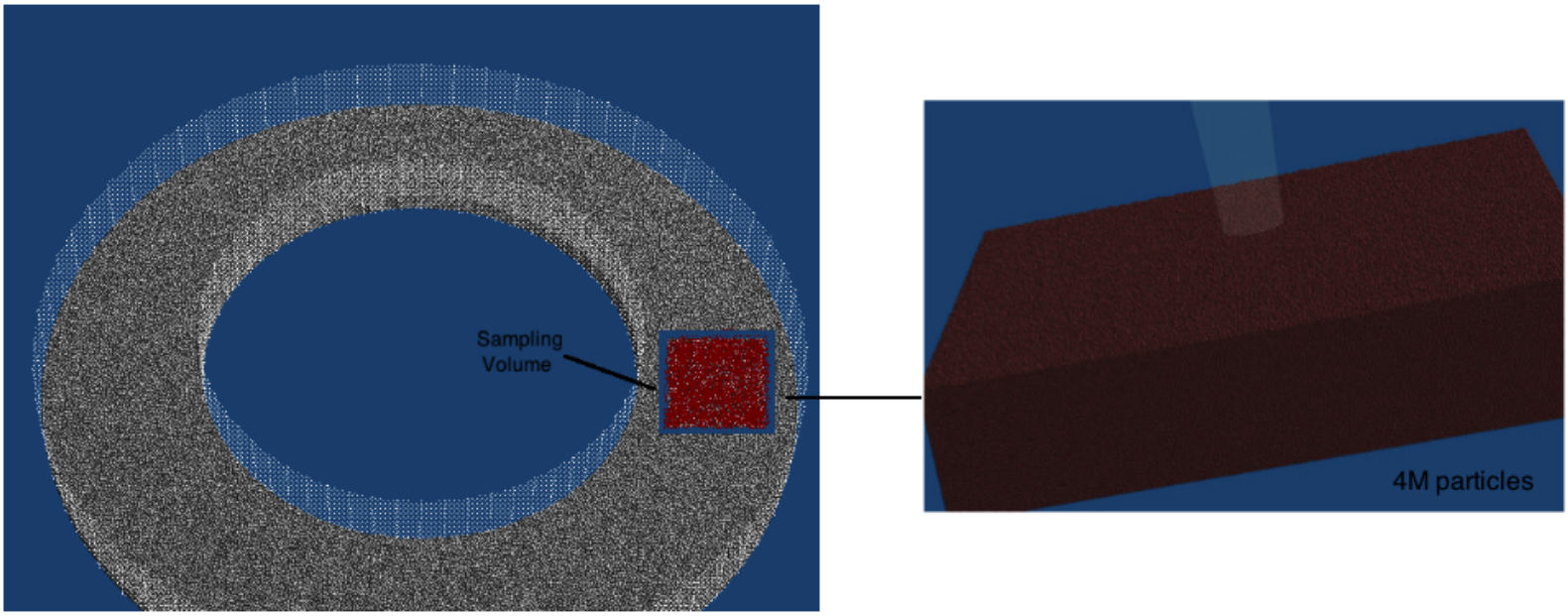

Figure 4.4: The rotary container - Sampling volume definition (left), Simulation of 4 Million particles in the sampling volume (right)

The amount of memory provided by the graphics card equipped, allowed the visualization of maximum 4 million particles. Fitting this number of particles in the whole container, would not offer any benefit, considering the fact that the region of interest was one representative sampling volume. Instead, a section of the whole container was selected, to define one sampling volume, where 4 million particles were simulated. This was achieved by scaling the dimensions of the dosator by a scale factor of 7, while retaining the dimensions of the simulation box constant (were the length of the simulation box equals the outer diameter of the container). The 4 million particles settling under gravity, formed a powder bed with a hight of 8 mm.

A normal diameter distribution of the generated particles was defined, modeling a standard powder, Lactohale 100, one to one. Image Analysis measurements on a sample of Lactohale 100, returned a Volume Mean Diameter (VMD) equal to approximately 0.16 mm. 4 million particles of the product Lactohale 100 correspond to approximately 11 grams of product. Considering the mean diameter and the variance of the distribution provided by these measurements, a respective diameter distribution for 4 million spherical particles was defined in the simulation. The diameter of the simulated particles covered a range between 0.1 mm to 0.22 mm, with mean diameter 0.16 mm. Concluding, a sample volume of approximately 13 cm^3 was filled with 4 million particles of a diameter distribution, identical to the particle size distribution of the standard powder Lactohale 100, achieving a realistic simulation:

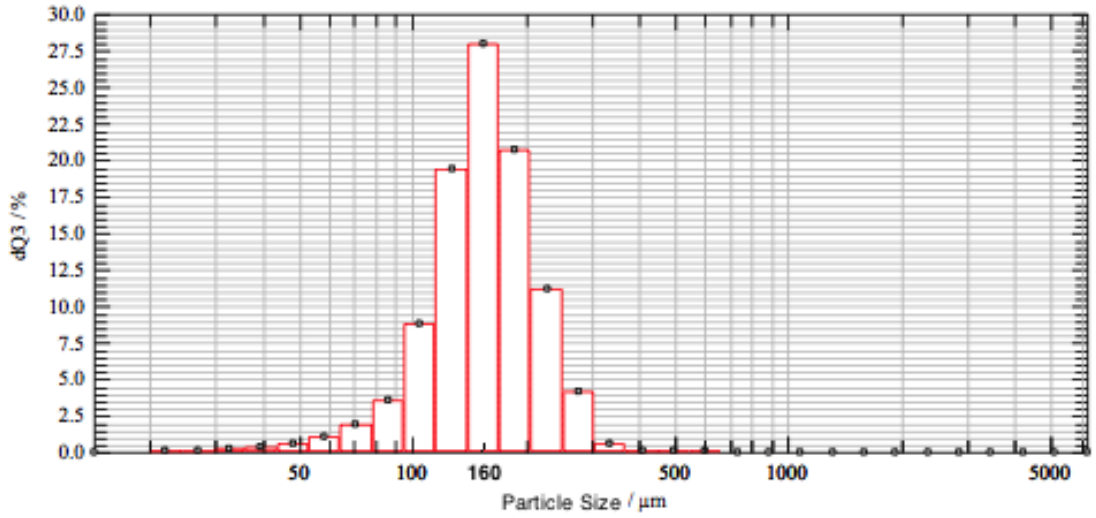

Figure 4.5: Particle size distribution(in micrometers) of Lactohale LH100, measured via microscopic image analysis. Particle size: diameter of a circle of equal projection area of the particle.

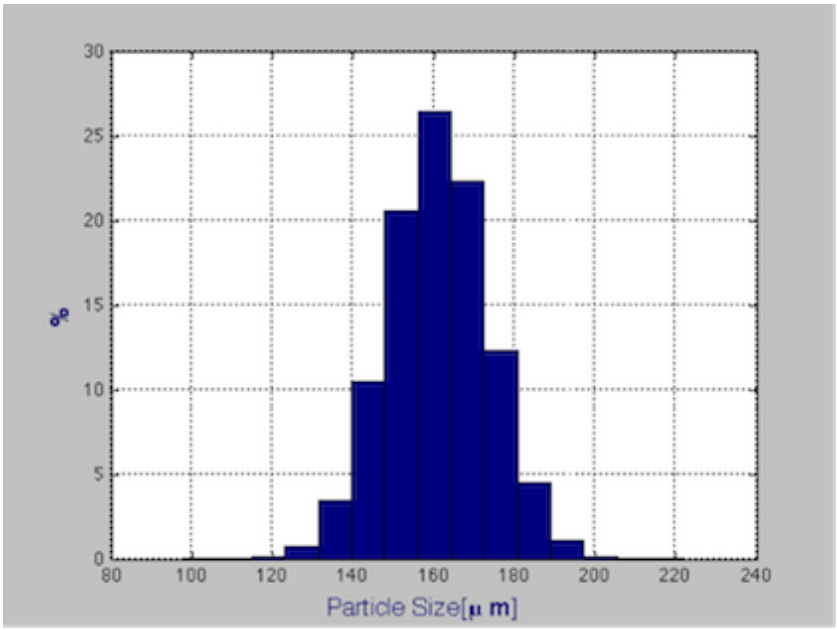

Figure 4.6: Particle diameter distribution (in micrometers), obtained by the simulation.

The simulation followed the following sequence of process steps:

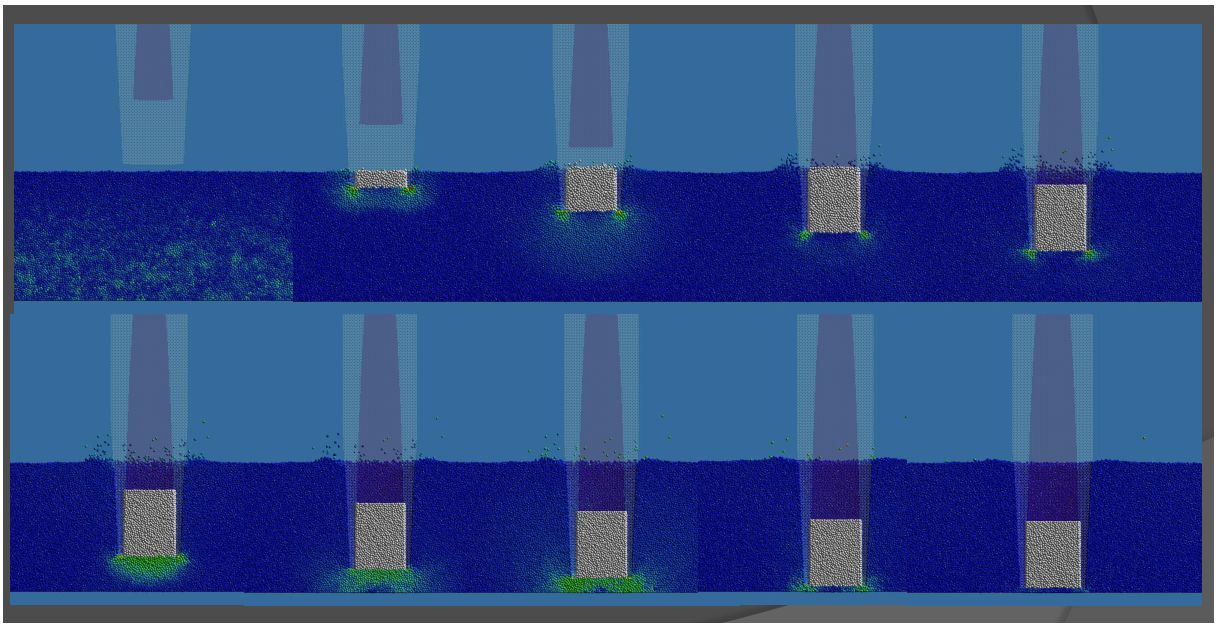

Figure 4.7: Snapshots from the simulation
(ratio of dosing chamber to powder Bed height = 1/2)

In comparison to the process steps described in paragraph 2.2.2, for the MG2-PLANETA capsule filling machine, here, the process steps of the MG2-LABBY were simulated. The only difference is that the size of the dosing chamber is set in advance, so the dosing tube and the piston move always simultaneously. The process was simulated only until the end of the descent of the dosator, when the final dosage is obtained. It should be mentioned that the dosator never reaches the bottom of the container. There is intentionally a small gap of 0.3 mm, between the base of the container and the lowest hight of the dosator. The influence of the gap on the uniformity of the powder bed was discussed in [30].

In figure 4.1, the blue colored particles are theoretically resting under gravity. In the code this means that for a blue particle, $\frac{E_{i,kinetic}(t)}{E_{i,potential}(t)} \ll 1$. The higher the ratio $\frac{E_{i,kinetic}(t)}{E_{i,potential}(t)}$ of a particle i, the warmer the color assigned to it. The simulation ends when $\frac{E_{kinetic}(t_{end})}{E_{potential}(t_{end})} \ll 1$, with $\frac{E_{potential}(t_{end})}{E_{kinetic}(t_{end})} < 10^9$.

5 Results

The objectives of the simulation, were: 1. to evaluate the energy fluctuations on the powder bed, during the sampling procedure, in order to study the powder bed uniformity. 2. to estimate the volume number density of the sampled powder, in order to study the capsule fill weight. Two operational parameters were examined:

process speed (dosator's speed):
Obviously, the higher the sampling time, the lower the process speed, for a constant dosator displacement. For this, the process speed was examined by defining eleven different computational sampling times st:

st	0.8	1.2	1.6	2.0	2.4	2.8	3.2	3.6	4.0	4.4	4.8

dosing chamber size:
The second operational parameter examined, was the size of the dosing chamber. The hight H, of the powder bed is constant. The ratio $\frac{Ch_k}{H}$ of four different chamber sizes $Ch_k, i = 1...4$ to the powder bed height H, was considered:

$\frac{Ch1}{H}$	$\frac{Ch2}{H}$	$\frac{Ch3}{H}$	$\frac{Ch4}{H}$
1/4	1/3	1/2	2/3

5.1 Effect of process speed on capsule fill weight

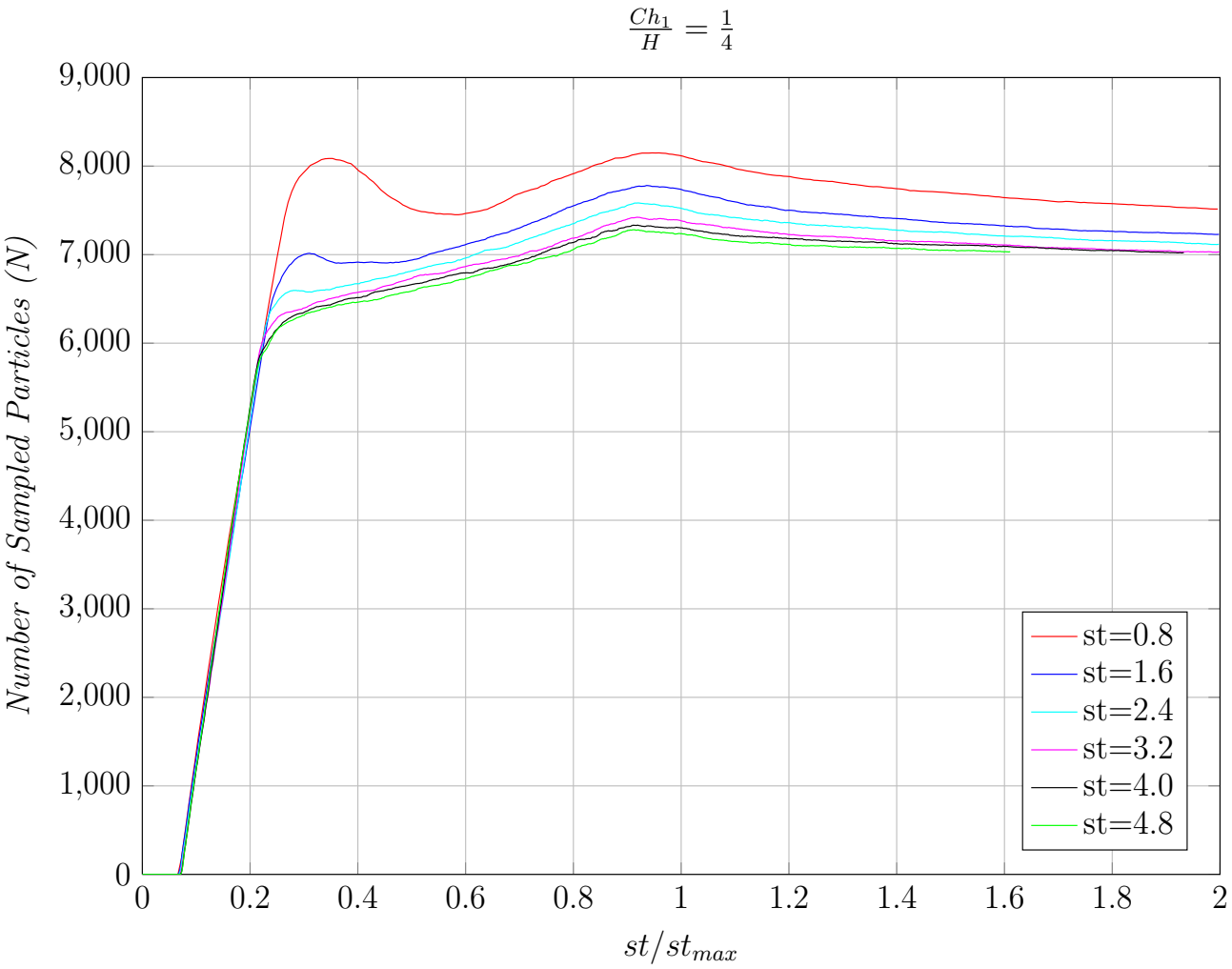

Figure 5.1: The number of sampled particles in the dosing chamber, over the normalized simulation time st/st_{max}, with ratio, $\frac{Ch_1}{H} = \frac{1}{4}$, for six different simulation times st.

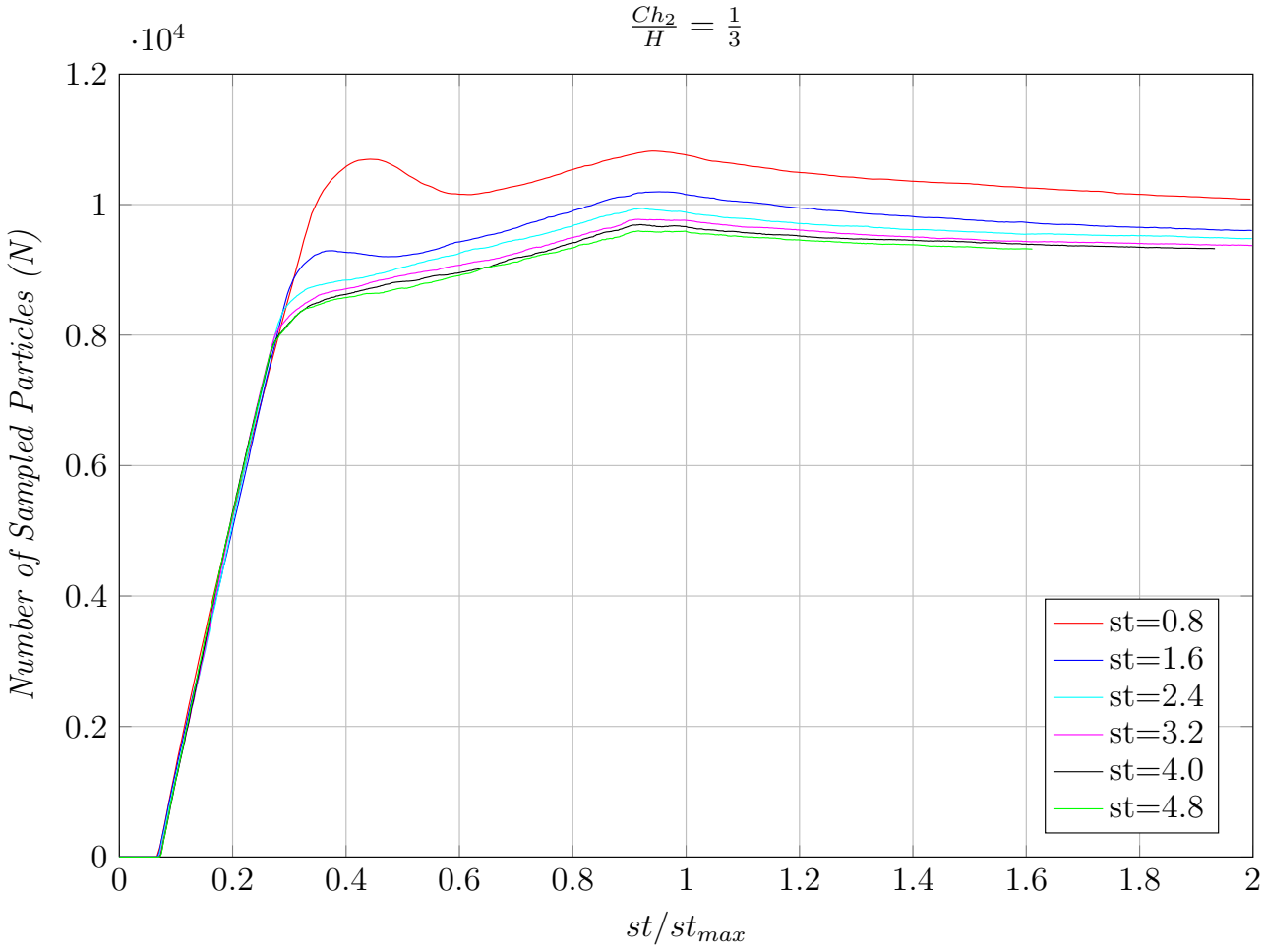

Figure 5.2: The number of sampled particles in the dosing chamber, over the normalized simulation time st/st_{max}, with ratio, $\frac{Ch_2}{H} = \frac{1}{3}$, for six different simulation times st.

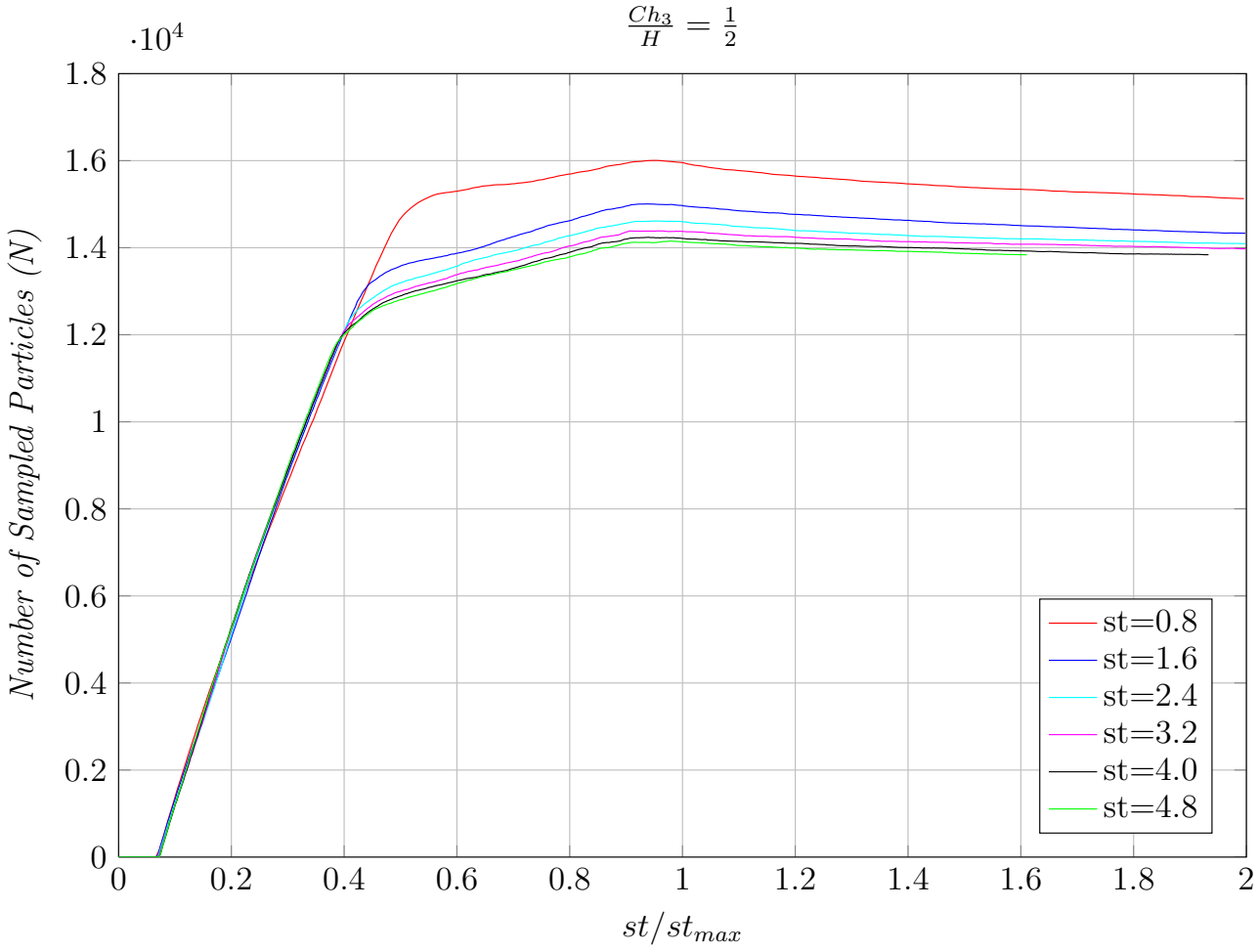

Figure 5.3: The number of sampled particles in the dosing chamber, over the normalized simulation time st/st_{max}, with ratio, $\frac{Ch_3}{H} = \frac{1}{2}$, for six different simulation times st.

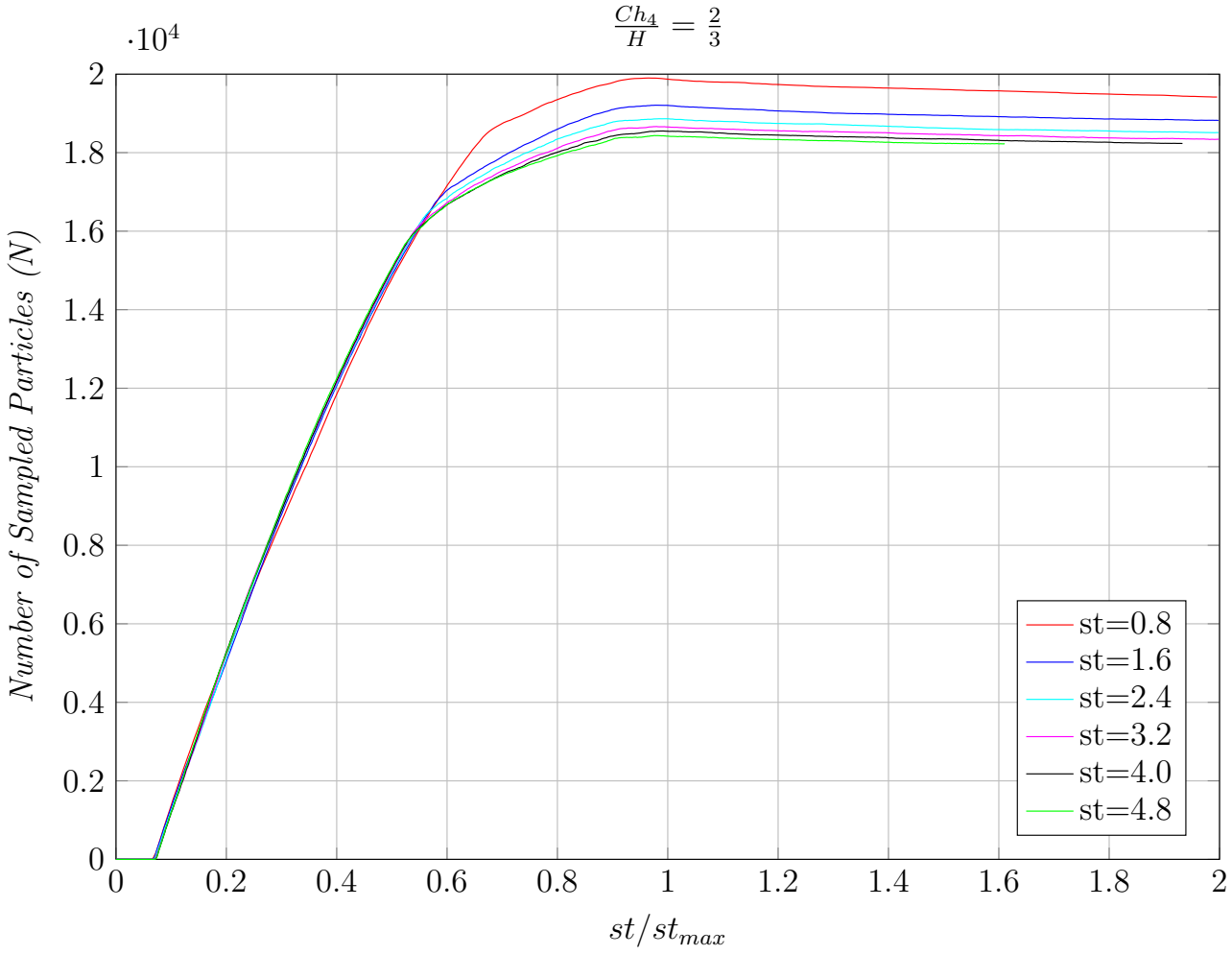

Figure 5.4: The number of sampled particles in the dosing chamber, over the normalized simulation time st/st_{max}, with ratio, $\frac{Ch_4}{H} = \frac{2}{3}$, for six different simulation times st.

In figures 5.1, 5.2, 5.3, 5.4, it can be observed how the velocity of the dosator while sampling, affects the volume number density of the final obtained dosage of product.

Volume number density:

$$n = \frac{N}{V_k} \tag{5.1}$$

Where, N the number of sampled particles and V_k, k = 1,...,4, is the volume of the dosing chamber Ch_k, k=1,...4, respectively, which corresponds to the four ratios Ch_k/H, k=1,...,4 previously defined. As observed in figures 5.1, 5.2, 5.3, 5,4, while increasing the velocity of the dosator (or decreasing the simulation sampling time st), the number of sampled particles N,overtime, in a set Volume V_k of the Ch_k dosing chamber,increases. Consequently, higher process speeds, result in increased capsule fill weights.

Moreover,it is observed, that for a specific dosator velocity (or simulation sampling time st), the number of sampled particles, increases overtime until $st/st_{max} = 1$. That is the time that the dosator reaches each final position of descent.

For $1 < st/st_{max} < 2$, the number of particles slightly decreases. During that period of time, the dosator stops moving, but the simulation continues running until the particles rest under gravity (refer to page 35), considering the fact that this is not a real time simulation. The gap between the powder bed and the final dosator position, allows some of the particles to escape from the chamber. This is particularly interesting for capsules produced for inhalation applications, because a more densified compacted plug is not desirable.

5.2 Effect of process speed on the powder bed uniformity (in terms of the total kinetic energy on the sampling volume)

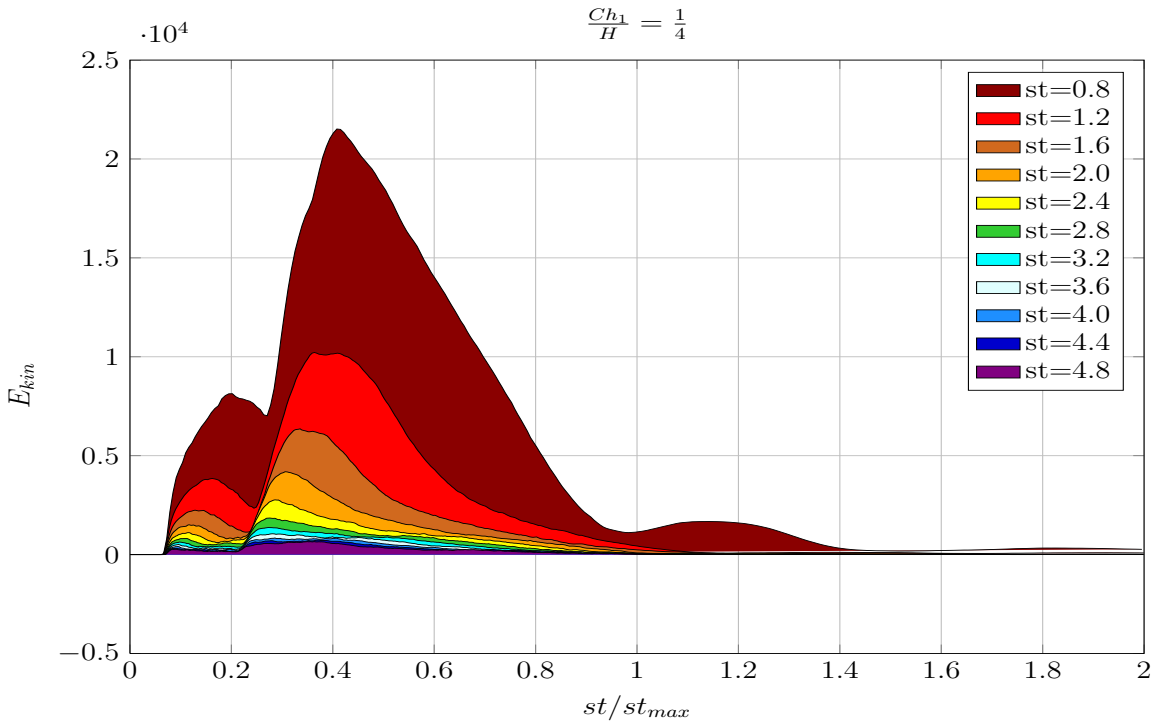

Figure 5.5: The total kinetic energy on the sampling volume, over the normalized simulation time st/st_{max} with ratio, $\frac{Ch_1}{H} = \frac{1}{4}$, for different simulation times st.

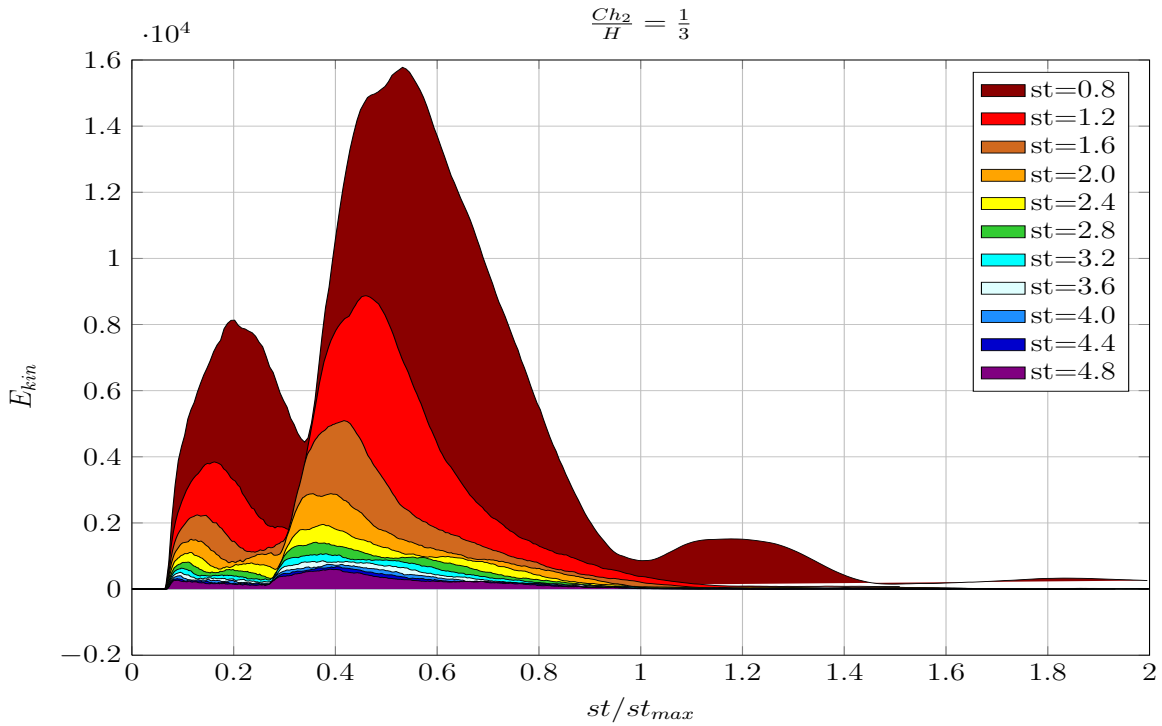

Figure 5.6: The total kinetic energy on the sampling volume, over the normalized simulation time st/st_{max} with ratio, $\frac{Ch_1}{H} = \frac{1}{3}$, for different simulation times st.

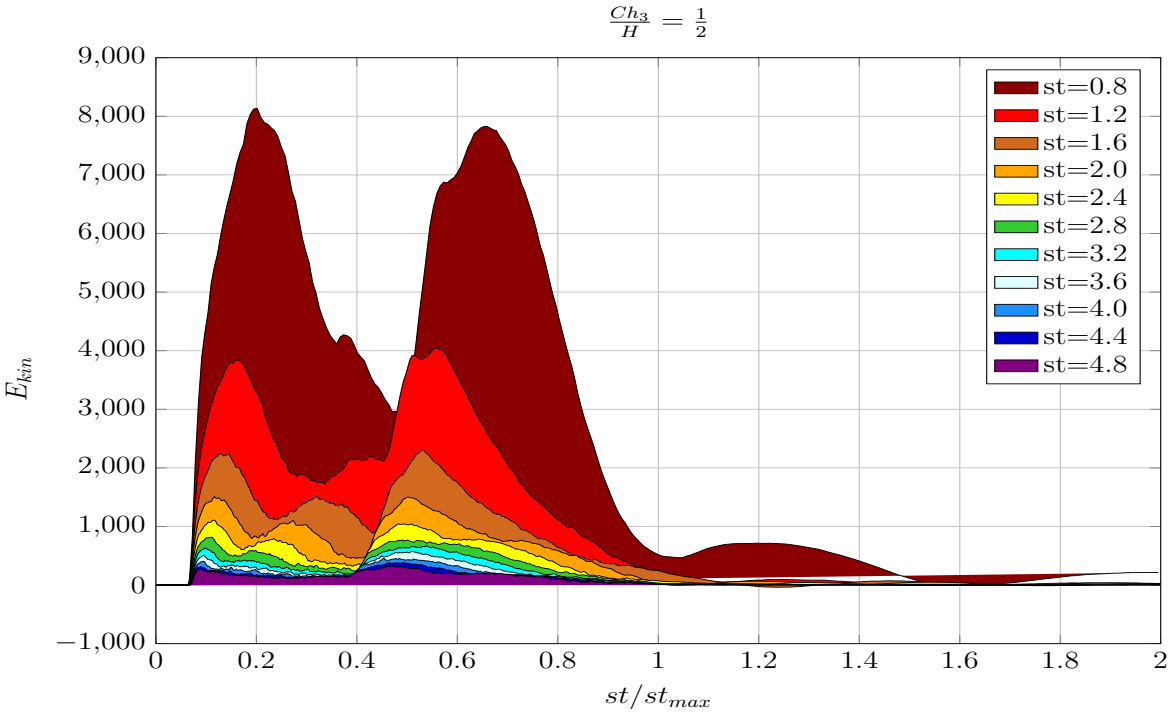

Figure 5.7: The total kinetic energy on the sampling volume, over the normalized simulation time st/st_{max} with ratio, $\frac{Ch_1}{H} = \frac{1}{2}$, for different simulation times st.

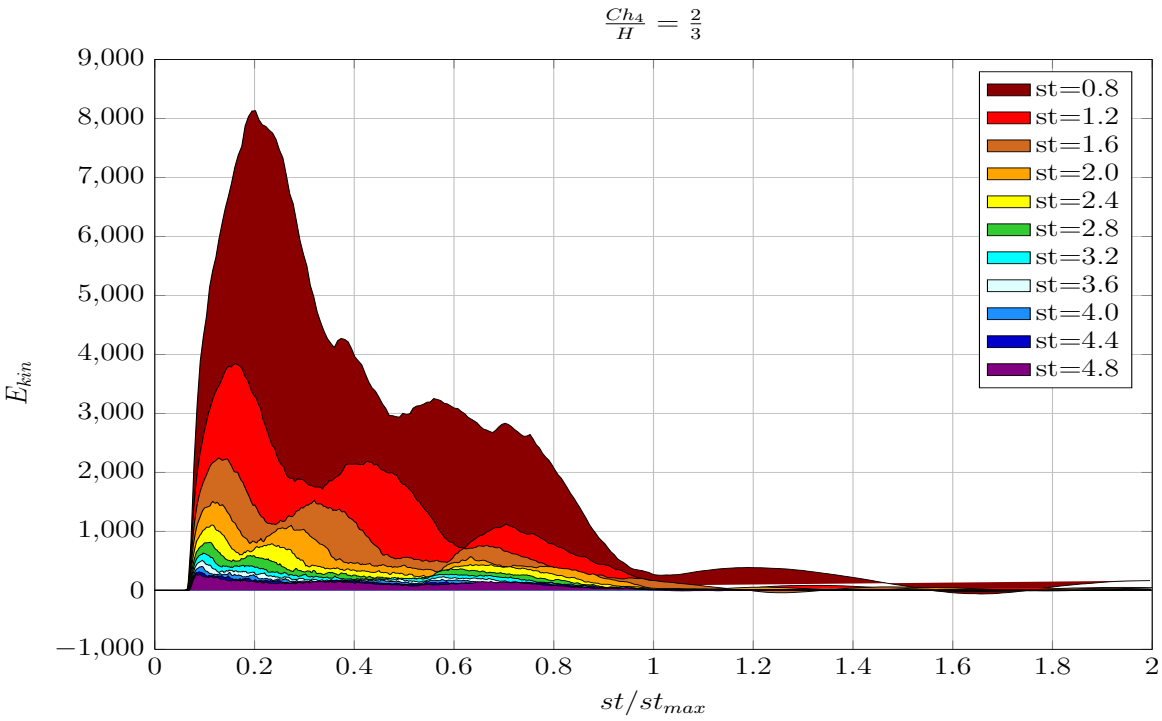

Figure 5.8: The total kinetic energy on the sampling volume, over the normalized simulation time st/st_{max} with ratio, $\frac{Ch_1}{H} = \frac{2}{3}$, for different simulation times st.

At each of the figures 5.5, 5.6, 5.7, 5.8, a qualitative interpretation of the kinetic energy overtime is given and it can be observed, that while lowering the sampling time st and as a consequence, rising the velocity of the dosator, the total kinetic energy on the sampling volume is increasing. The kinetic energy fluctuations on the sampling volume lead to fluctuations in the bulk density of the powder [31], and after repeated sampling, the uniformity of the whole powder bed is affected. Thus, from the above results it can be claimed, that higher process speeds lead to a less uniform powder bed.

Moreover, the following figure interprets how the kinetic energy is fluctuating over the sampling time and its progress at every step of the filling process:

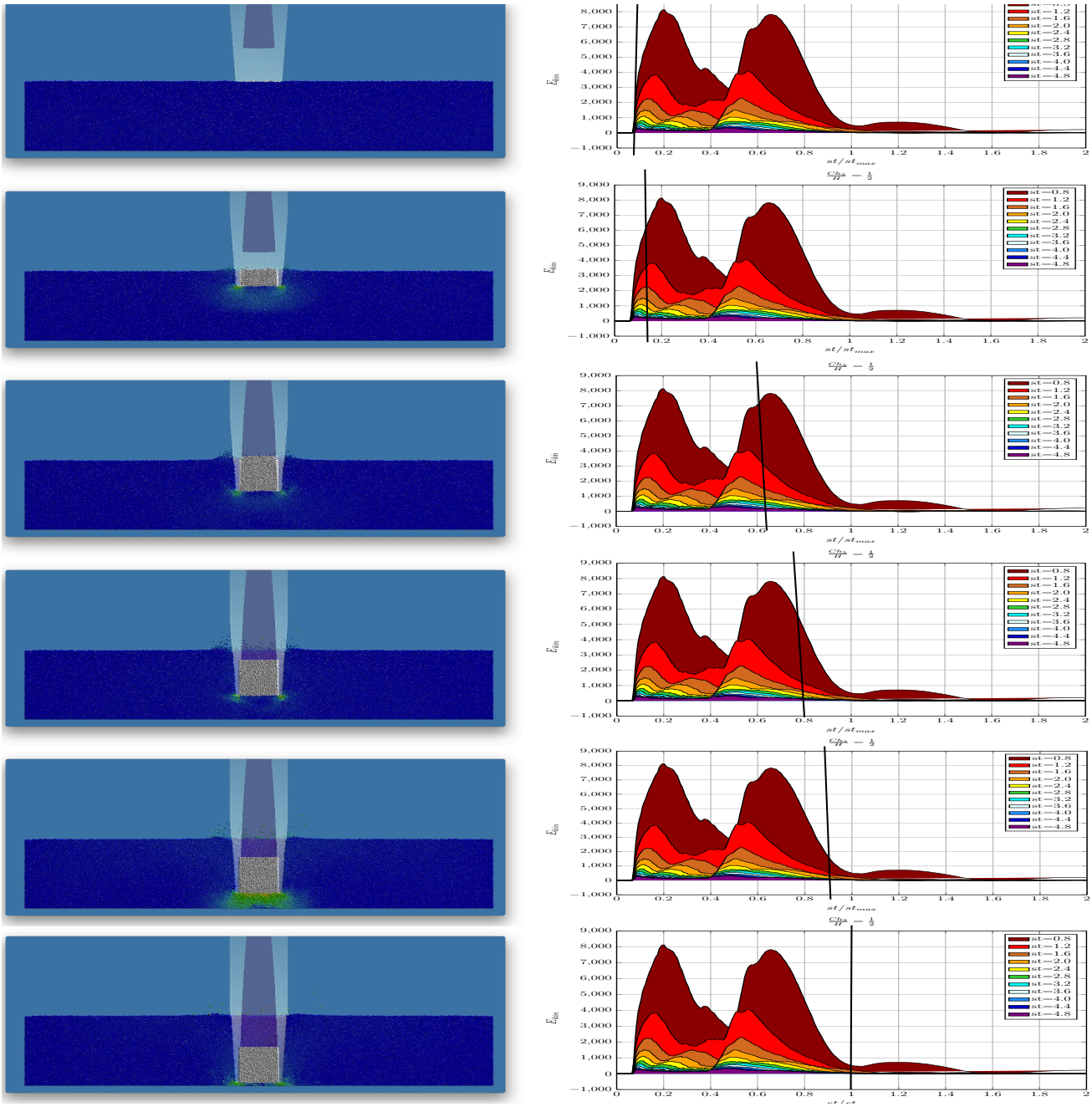

Figure 5.9: The simulation time steps (left) in respect to the kinetic energy overtime (right)

5.3 Effect of dosing chamber size on the powder bed uniformity (in terms of the total kinetic energy on the sampling volume)

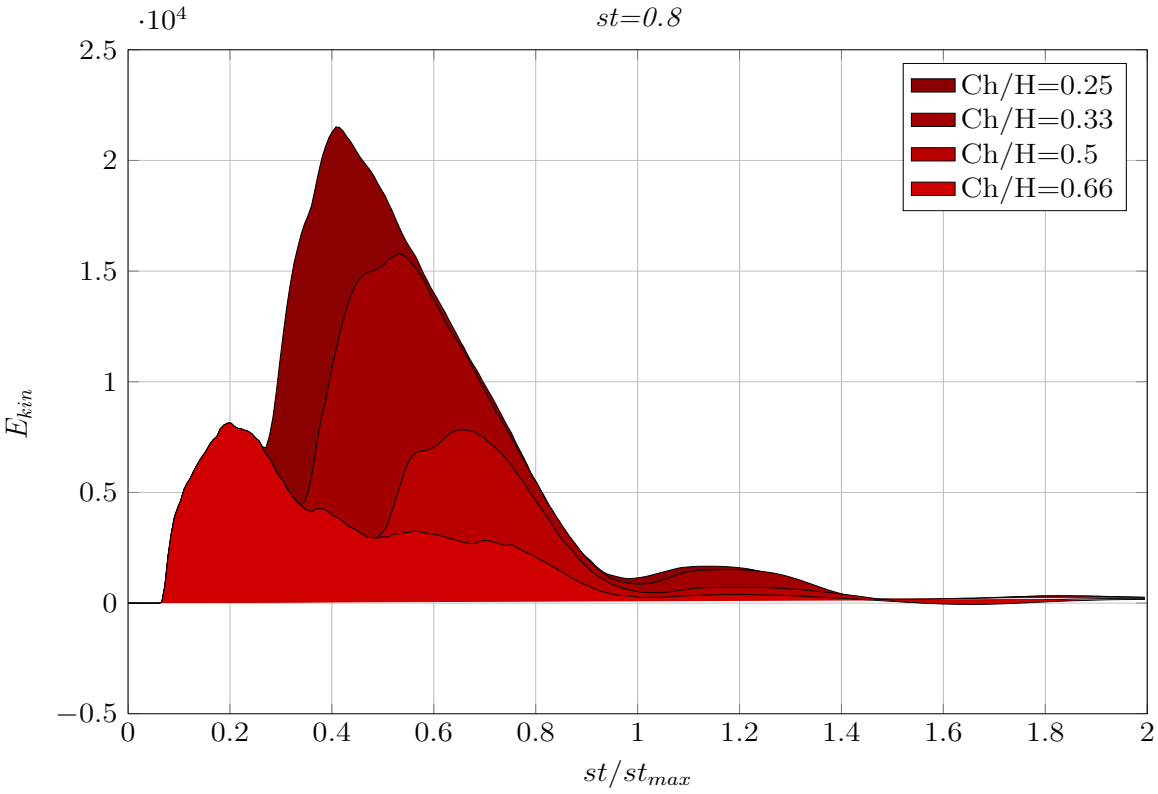

Figure 5.10: The total kinetic energy on the sampling volume, over the normalized sampling time st/st_{max}, for $st = 0.8$ and four different ratios $\frac{Ch}{H}$.

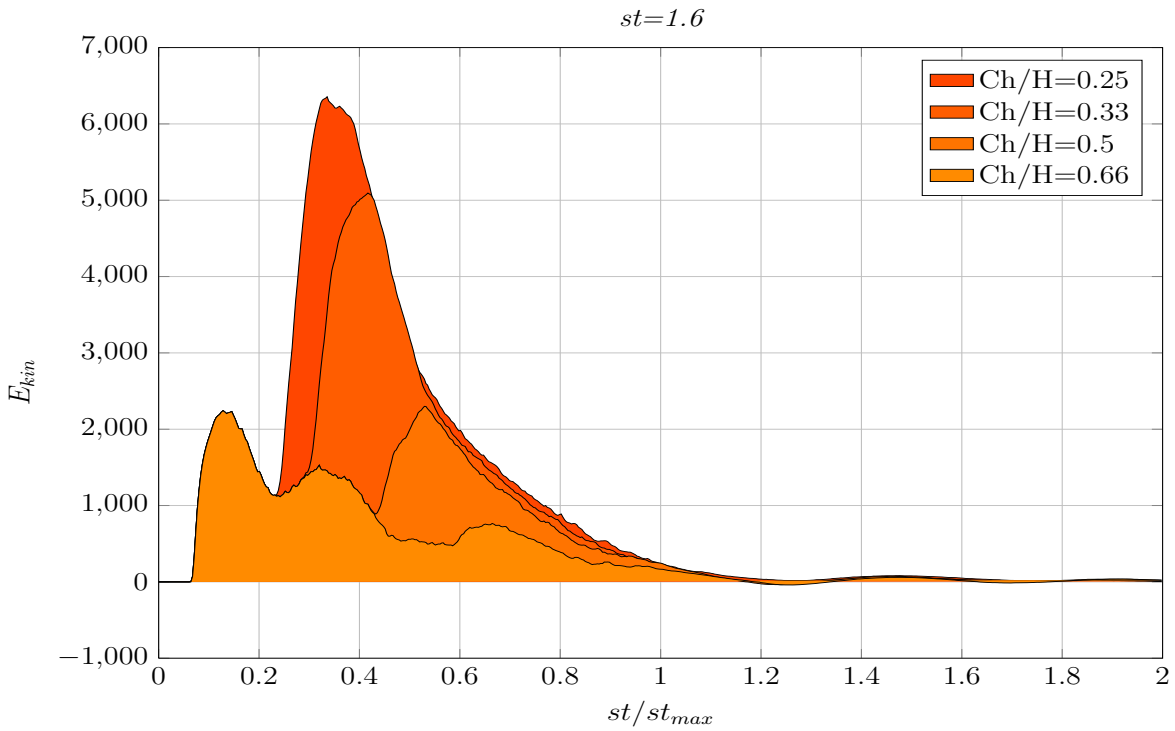

Figure 5.11: The total kinetic energy on the sampling volume, over the normalized sampling time st/st_{max}, for $st = 1.6$ and four different ratios $\frac{Ch}{H}$.

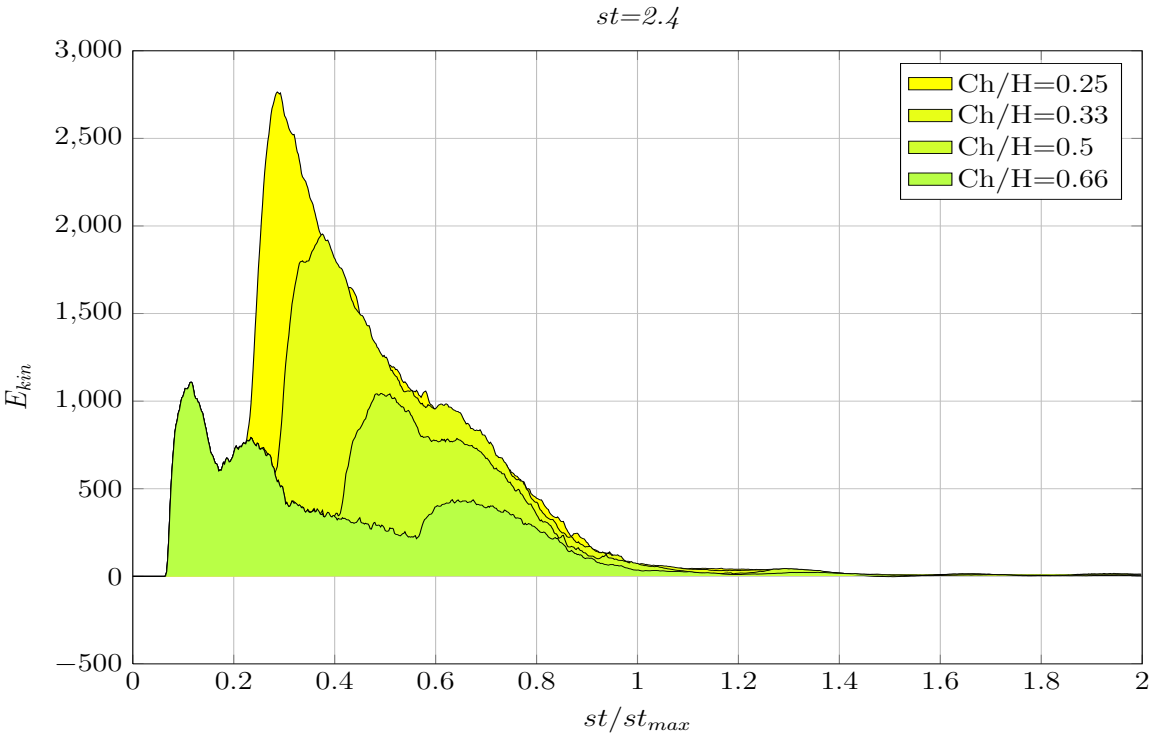

Figure 5.12: The total kinetic energy on the sampling volume, over the normalized sampling time st/st_{max}, for $st = 2.4$ and four different ratios $\frac{Ch}{H}$.

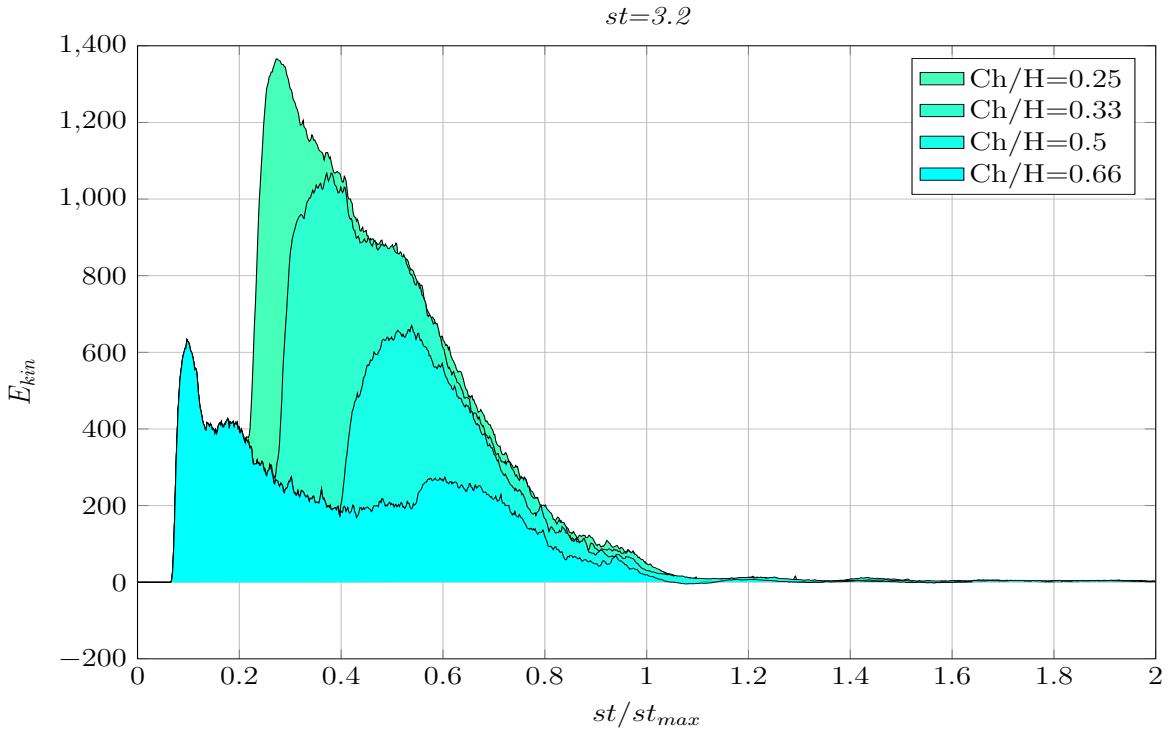

Figure 5.13: The total kinetic energy on the sampling volume, over the normalized sampling time st/st_{max}, for $st = 3.2$ and four different ratios $\frac{Ch}{H}$.

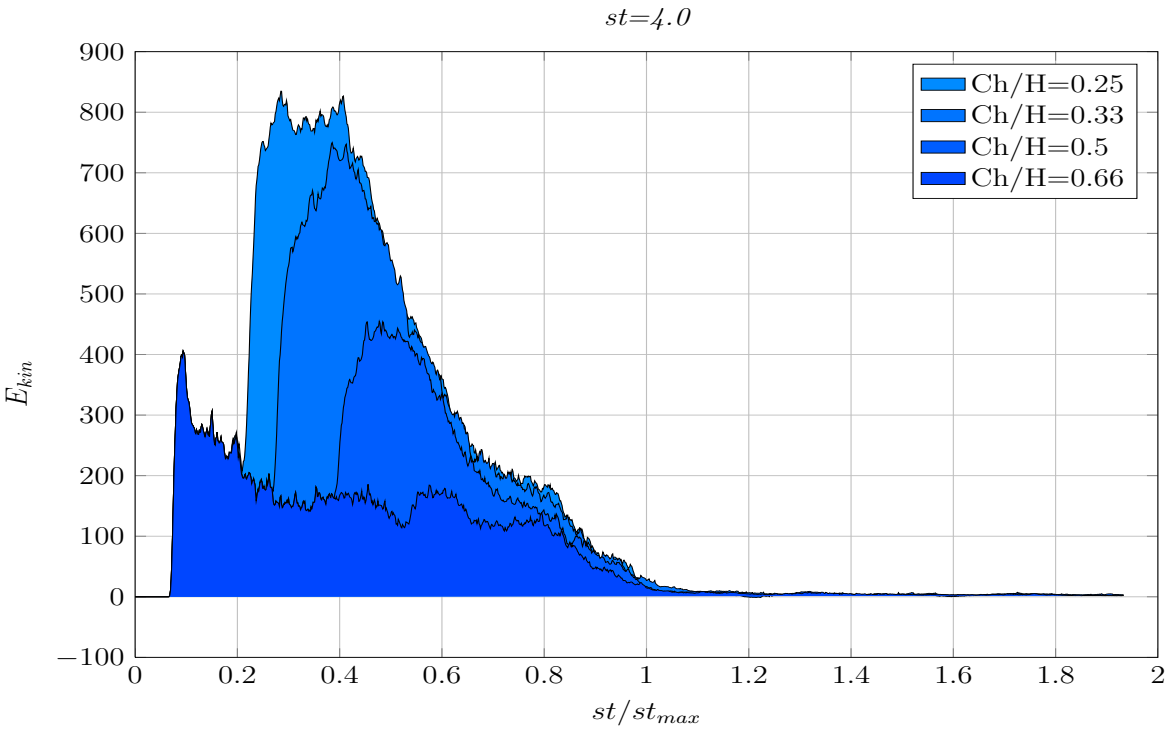

Figure 5.14: The total kinetic energy on the sampling volume, over the normalized sampling time st/st_{max}, for $st = 4.0$ and four different ratios $\frac{Ch}{H}$.

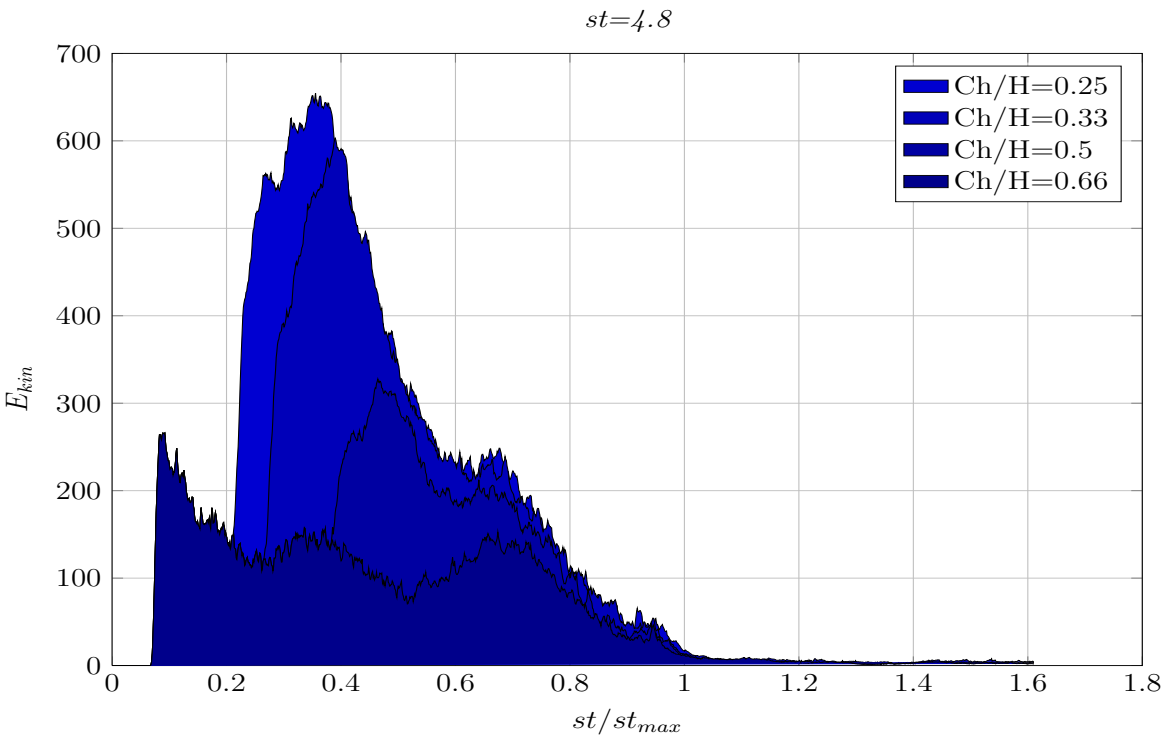

Figure 5.15: The total kinetic energy on the sampling volume, over the normalized sampling time st/st_{max}, for $st = 4.8$ and four different ratios $\frac{Ch}{H}$.

A qualitative analysis of the total kinetic energy on the sampling volume depending on the size of the dosing chamber is interpreted in figures 5.10, 5.11, 5.12, 5.13, 5.14 and 5.15, for different process speeds respectively in each figure. Results saw that the kinetic energy is rising while the dosing chamber size decreases. The kinetic energy on the powder bed is used here to measure the distortion noticed on the powder bed. The higher the kinetic energy the higher the level of distortion, thus the less the uniformity. This allows to claim that the larger the dosing chamber, the more uniform the powder bed.

6 Conclusion and future work

The objective of this thesis was the simulation of an automatic capsule filling process, using a discrete element method (DEM) code parallelized with the parallel computing architecture CUDA, to model the particulate system of a pharmaceutical powder. The motivation derived from the fact, that in some cases, the fill weights of the obtained capsules are inconstant, leading to failure in obtaining equal doses in each capsule. There are various factors that could lead to such dose inconsistencies, including material properties, equipment design and operational parameters. This thesis was focused on the investigation of two operational parameters. Because of the fact that there are also other factors affecting the fill weight variability, the results obtained, were only individual observations. They could be combined with future results obtained by further studies on material properties, or studies on different operational parameters.

The conclusions were the following: 1. Higher process speeds result in increased capsule fill weights and could have a positive effect on the consistency of the doses obtained. 2. Very high process speeds could have a negative effect on the uniformity of the powder bed. 3. Very small dosing chambers could have a negative effect on the uniformity of the powder bed.

References

[1] Fridrun Podczeck and Brian E Jones: *Pharmaceutical Capsules*, 2nd Edition, Pharmaceutical Press 2004.

[2] Khan, A. S. and Huang, S. (1995): *Continuum theory of plasticity*, John Wiley & Sons, New York.

[3] Bardet, J.P., Vardoulakis, I. (2001): *The asymmetry of stress in granular media*, Int. J. Solids Struct. 38, 353Ð367

[4] Sergio H. Faria et. al (2014): *Continuum Description of Granular Materials*, JSpringer; 2014 edition

[5] F. Goncu (2012): *Mechanics of Granular Materials: Constitutive Behavior and Pattern Transformation*, Ipskamp Drukkers, Enschede, The Netherlands

[6] N.C.Markatos and D.Kirkcaldy(1983) ,*Analysis and computation of 3D,transient flow and combustion through granulated propellants*,Int.J.Heat/Mass Transfer,vol. 26,no.7,1037-1053,1983

[7] N.C Markatos(1986) ,*Modelling of two-phase transient flow and combustion of granulated propellants*, Int.J.of Multi-Phase Flow, vol12,6,913-933,1986

[8] Feda, J. (1982): *Mechanics of particulate materials. Development in geotechnical engineering*, Elsevier publisher, Amsterdam.

[9] Malvern, L. (1969): *Introduction to the mechanics of a continuous medium.*, Prentice- Hall, Inc., Englewood Cliffs, New Jersey.

[10] Cundall, P. A. (1971): *A computer model for simulating progressive, large- scale movements in blocky rock systems*, Proc. Symp. Int. Soc. Rock Mech., Nancy, 2, 132

[11] Cundall, P. A. (1978): *BALL-A computer program to model granular media using the distinct element method*, Technical note TN-LN-13, Advance Technology Group, Dames and Moore, London.

[12] Cundall, P. A. and Strack (1979a): *The development of constitutive laws for soil using the distinct element method*, Third International Conference on Numerical Methods in Geomechanics, Wittke (Eds), Balkema, Aachen, 289-298

[13] Cundall, P. A. and Strack (1979b): *A discrete numerical model for granular assemblies*, Geotechnique, 29(1), 47-65.

[14] Williams, J.R., Hocking, G., and Mustoe, G.G.W. (1985): *The Theoretical Basis of the Discrete Element Method*, NUMETA 1985, Numerical Methods of Engineering, Theory and Applications, A.A. Balkema, Rotterdam, January 1985

[15] Shi, G (1989): *Discontinuous deformation analysis Ð A new numerical model for the statics and dynamics of deformable block structures,* In 1st U.S. Conf. on Discrete Element Methods, Golden. CSM Press: Golden, CO, 1989.

[16] Jidong Zhao, Tong Shan(2013): *Coupled CFDÐDEM simulation of fluidÐ particle interaction in geomechanics*, Powder Technology, Volume 239, May 2013, Pages 248Ð 258

[17] Dalibor Jajcevic, et. al (2013): *Large-scale CFDÐDEM simulations of fluidized granular systems*, Chemical Engineering Science, Volume 98, 19 July 2013, Pages 298-310

[18] Daoyin Liu, et. al (2013): *Development and test of CFD - DEM model for complex geometry: A coupling algorithm for Fluent and DEM*, Computers & Chemical Engineering, Volume 58, 11 November 2013, Pages 260-268

[19] William R. Ketterhagen, et. al(2008): *Process Modeling in the Pharmaceutical Industry using the Discrete Element Method*, Journal of Pharmaceutical Sciences, Vol. 98, 442Ð470 (2009)

[20] J. M. Boac, et. al(2010): *Material and Interaction Properties of Selected Grains and Oilseeds for Modeling Discrete Particles*, American Society of Agricultural and Biological Engineers, Vol. 53(4): 1201-1216

[21] Charles A. Radeke, et. al (2010): *Large-scale Mixer Simulations Using Massively Parallel GPU Architectures*, Chemical Engineering Science (01 October 2010)

[22] Jodrey W. S., Tory E. M., (1979): *Simulation of random packing of spheres*, J. Simulation 32, 1 - 12 (1979).

[23] odrey W. S., Tory E. M.,(1985): *Computer Simulations of close random packing of equal spheres*, Physical Review A.32.3247.

[24] Stoyan D., (2002): *Simulation and characterization of random systems of hard particles.*, Image Anal. Stereol. 21, S41 - S48

[25] M. P. Allen and D. J. Tildesley (1989): *Computer Simulation of Liquids*, Clarendon Press

[26] Walton, O. R. (1983): *Application of molecular dynamics to macroscopic particles*, Int. J. Eng. Sci.,22, 1097-1107

[27] Cundall, P. A. and Strack (1979): *A discrete numerical model for granular assemblies*, Geotechnique 29: 47- 65

[28] Lee J. (1994): *LDensity waves in the flows of granular media.*, Ind Eng Chem Res 43:5521Ð5528.

[29] ZhangJ, et. al (2004): *Application of the discrete approach to the simulation of size segregation in granular chute flow.*, Chemical Engineering Science (01 October 2010)

[30] Angulo Pinzon, Oscar Andres (2012): *Modelling of dosator filling and discharge*, PhD thesis, University of Greenwich.

[31] Woodhead P. J (1980): *The Influence of Powder Bed Porosity Variations on the Filling of Hard Gelatin Capsules by a Dosator System*, PhD thesis, University of Nottingham .